

Bis-alkylamine Indolo[3,2-*b*]quinolines as Hemozoin Ligands: Implications for Antimalarial Cytostatic and Cytocidal Activities

Alexandra Paulo,^{*,†} Marta Figueiras,[†] Marta Machado,[‡] Catarina Charneira,[†] João Lavrado,[†] Sofia A. Santos,[†] Dinora Lopes,[‡] Jiri Gut,[§] Philip J. Rosenthal,[§] Fátima Nogueira,[‡] and Rui Moreira[†]

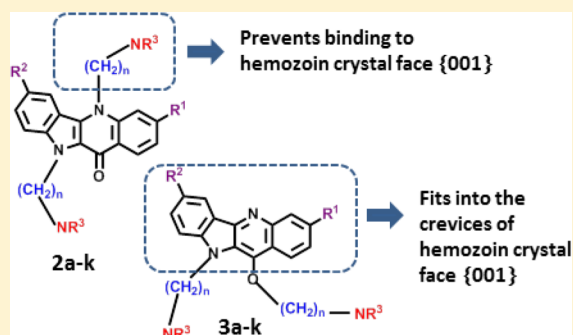
[†]Instituto de Investigação do Medicamento (iMed.Ulisboa), Faculdade de Farmácia, Universidade de Lisboa, Av. Prof. Gama Pinto, 1649-003 Lisboa, Portugal

[‡]UEI Malaria, Centro da Malária e Doenças Tropicais, IHMT, Universidade Nova de Lisboa, Rua da Junqueira, 100, P-1349-008 Lisboa, Portugal

[§]Department of Medicine, San Francisco General Hospital, University of California, San Francisco, Box 0811, San Francisco, California 94143, United States

S Supporting Information

ABSTRACT: To get insight into the relevance of targeting hemozoin (Hz) crystals, two isomeric series, N5,N10-bis-alkylamine (**2a–k**) and N10,O11-bis-alkylamine (**3a–k**) indolo[3,2-*b*]quinolines, were evaluated for their in vitro activity against chloroquine (CQ)-resistant and sensitive strains of *Plasmodium falciparum*. In general, compounds of series **3** were more active than isomers **2**, with IC₅₀/LD₅₀ ranging from 25/233 nM (**3i**) to 1.3 (**3a**)/10.7 (**3b**) μM. SAR analyses showed that lipophilicity and chlorine substitution at C3 increased both cytostatic and cytotoxic activities. Both series bound to hematin monomer, inhibited β-hematin formation in vitro, delayed intraerythrocytic parasite development with apparent inhibition of Hz biocrystallization, and showed higher cytotoxic activity against schizonts. In addition, cytostatic and cytotoxic activities of series **3**, but not those of isomers **2**, correlated with calculated vacuole accumulation ratios, suggesting different capacities of **2** and **3** to bind to the Hz crystal face {001} exposed on the vacuole aqueous medium and different mechanisms of cytotoxic potency.



INTRODUCTION

Malaria, in particular infection with *Plasmodium falciparum*, the most lethal of the human malaria parasite species, is a global health problem. A major contributor to the problem is the emergence and spread of multidrug-resistant strains of *P. falciparum*. Despite continued attempts to develop a vaccine, current control of malaria depends on imperfect measures to control vector mosquitoes and the use of drugs to treat and prevent the disease.¹ Thus, there is an urgent need for novel drugs targeting parasite intraerythrocytic stages to treat infected individuals and, ideally, also to prevent transmission. The ideal drug or drug combination should be of single dose and able to clear from the body all parasite forms, in a short period of time.^{1,2} This implies that screening for new drug candidates should include cytotoxic assays (parasite viability assays after short drug bolus)³ and not only parasite growth inhibition screenings which do not guarantee the capacity of compounds to kill the parasite in a short period of time.

Malaria parasites have a complex life cycle, of which the erythrocytic stage is responsible for the diverse symptoms caused by infection. Inside erythrocytes, parasites ingest and digest 70–80% of host hemoglobin as an amino acid source, to maintain osmotic stability and to provide space for the

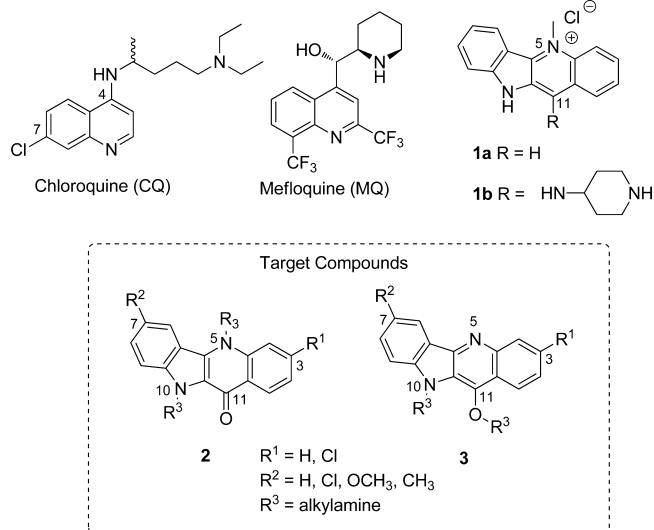
intracellular parasite.⁴ During this process, free heme is released as a toxic byproduct that is detoxified by a biomineralization process into a nontoxic crystal structure called hemozoin (Hz) or malarial pigment, present in asexual and sexual blood stages.^{5,4a,6} Hemoglobin degradation and Hz formation are essential for parasite survival, making these processes important targets for antimalarial drug development. Heme detoxification into Hz, believed to be the primary target of quinoline antimalarials such as chloroquine (CQ, Chart 1),⁷ remains one of the most attractive drug development targets, in part due to the immutable nature of heme. Resistance to CQ is associated with mutations in the gene encoding the digestive vacuole (DV) membrane protein *P. falciparum* chloroquine resistance transporter (PfCRT),⁸ which appears to result in reduced drug concentration at the target without altering the target itself. In this case, in contrast to drug resistance on the basis of protein target mutations, the target remains vulnerable and the organism susceptible to drug action if access and binding to the target can be achieved.

Received: December 2, 2013

Published: March 27, 2014



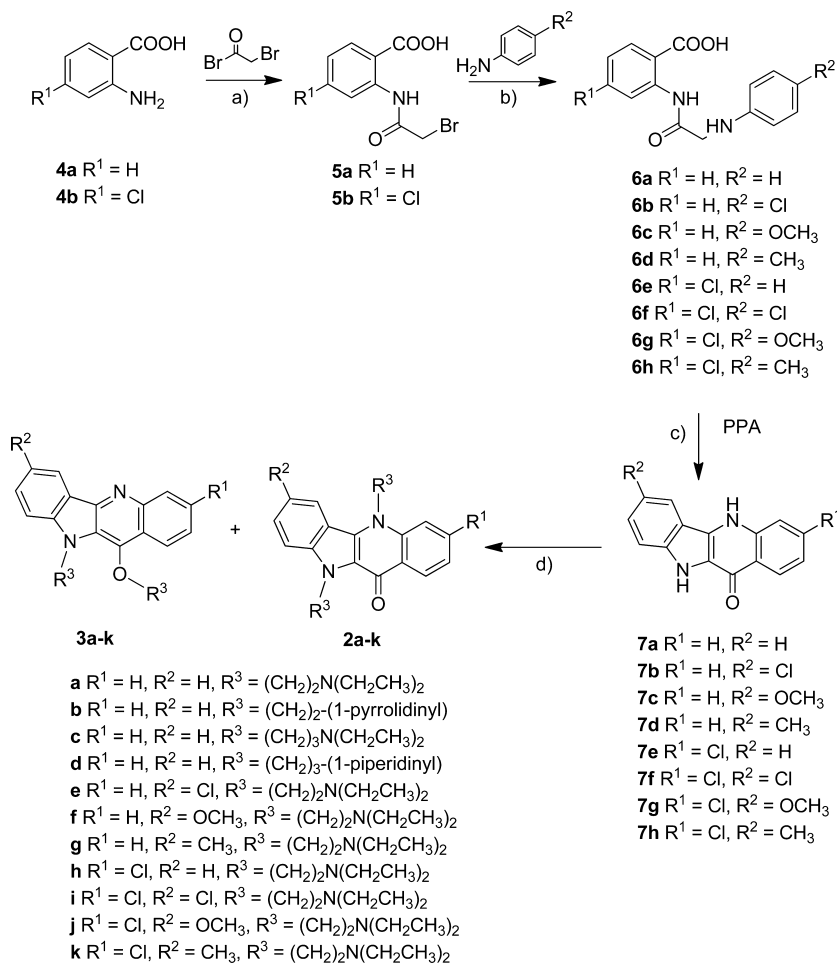
Chart 1. Structures of Chloroquine (CQ), Mefloquine (MQ), Cryptolepine (1a), Its C11-Aminoalkylamine Derivative 1b, and Bis-alkylamine Indolo[3,2-*b*]quinolines 2 and 3



Inhibition of H₂ formation by several antimalarials, including CQ, mefloquine (MQ; Chart 1), and amodiaquine, has long been proposed^{7a} but only recently shown to occur in the parasite.⁹ However, the mechanism of H₂ biocrystallization inhibition by these antimalarials is still a matter of debate. As recently reviewed,¹⁰ several studies indicate that they may inhibit H₂ crystallization by binding to the heme monomer,¹¹ or the μ -oxodimer,¹² or the “head-to-tail” dimer that is adsorbed on the crystal surface, or even by acting as capping molecules on H₂ crystal faces.^{7a,13} In addition, it was recently shown that in vitro drug–heme interactions leading to inhibition of formation of synthetic H₂ (β -hematin) by CQ and other related quinoline drugs correlated with parasite growth inhibition (cytostatic activity) but not with cytotoxic activity.¹⁴ Despite many studies of quinoline drug–heme interactions and their implications for disruption of heme monomer–dimer equilibria and inhibition of H₂ formation,¹⁰ our understanding of drug–hemozoin interactions remains sparse, even with the efforts made recently.¹⁵

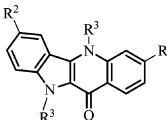
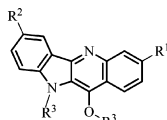
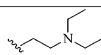
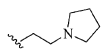
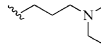
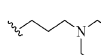
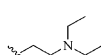
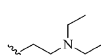
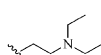
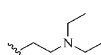
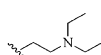
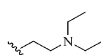
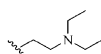
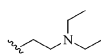
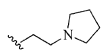
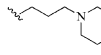
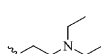
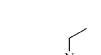
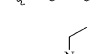
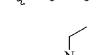
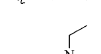
On the basis of the theoretical growth form of β -hematin,^{13a,b,16} it has been proposed that CQ might cap onto the corrugated fast-growing {001} H₂ surface via a salt bridge between the CQ side-chain amine and a heme propionic acid and still fit on that surface by intercalation of the quinoline ring

Scheme 1. Synthesis of Bis-alkylamine Indolo[3,2-*b*]quinolines 2a–k and 3a–k^a



^aReaction conditions: (a) DMF:1,4-dioxane (1:1), room temperature, overnight, 96–99% yield; (b) appropriate aniline, DMF, 120 °C, 18–96 h, 22–83% yield; (c) 130 °C, 2 h, 11–79% yield; (d) chloroalkylamine, dry acetone, K₂CO₃ NaI, reflux, 18–48 h, 20–35% yield.

Table 1. Cytostatic (IC₅₀) and Cytocidal (LD₅₀) Activities of Series 2 and 3, Chloroquine (CQ), and Artemisinin (Art) against *P. falciparum* CQ-Resistant Strains (W2 and Dd2) and CQ-Sensitive Strain 3D7 and Corresponding Resistance Indices (giRI and cRI)

	 2			 3					
				IC ₅₀ (μM) ± SD		LD ₅₀ (μM) ± SD			
	R ¹	R ²	R ³	PfW2	Pf3D7	PfDd2	Pf3D7	giRI ^a	cRI ^b
2a	H	H		0.702±0.139	2.52±0.087	2.34±0.485	10.5±3.17	0.3	0.2
2b	H	H		0.407±0.045	1.03±0.097	2.61±0.250	4.14±0.481	0.4	0.6
2c	H	H		0.344±0.017	1.65±0.091	n.d.	n.d.	0.2	n.d.
2d	H	H		0.167±0.022	0.497±0.002	n.d.	n.d.	0.3	n.d.
2e	H	Cl		0.416±0.043	1.01±0.002	n.d.	n.d.	0.4	n.d.
2f	H	OCH ₃		0.420±0.015	1.71±0.868	n.d.	n.d.	0.2	n.d.
2g	H	CH ₃		0.383±0.036	1.28±0.192	2.24±0.239	3.60±1.05	0.3	0.6
2h	Cl	H		0.254±0.027	0.737±0.132	n.d.	n.d.	0.3	n.d.
2i	Cl	Cl		0.153±0.001	0.329±0.076	0.674±0.121	0.460±0.115	0.5	1.4
2j	Cl	OCH ₃		0.207±0.063	0.917±0.022	n.d.	n.d.	0.2	n.d.
2k	Cl	CH ₃		0.257±0.073	0.848±0.092	n.d.	n.d.	0.3	n.d.
3a	H	H		0.533±0.028	1.27±0.122	n.d.	n.d.	0.4	n.d.
3b	H	H		0.460±0.040	1.10±0.079	7.49±1.09	10.7±2.42	0.4	0.7
3d	H	H		0.110±0.031	0.446±0.034	n.d.	n.d.	0.2	n.d.
3e	H	Cl		0.188±0.018	0.307±0.031	3.00±0.481	8.92±3.73	0.6	0.3
3h	Cl	H		0.101±0.009	0.346±0.008	4.62±0.364	2.93±0.997	0.3	1.6
3i	Cl	Cl		0.025±0.002	0.156±0.009	0.399±0.034	0.233±0.056	0.2	1.7
3j	Cl	OCH ₃		0.134±0.027	0.372±0.030	n.d.	n.d.	0.4	n.d.
3k	Cl	CH ₃		0.176±0.029	0.247±0.120	n.d.	n.d.	0.7	n.d.
CQ				0.065±0.005	0.009±0.004	9.04±2.86	0.079±0.019	7.0	113
Art				0.014±0.001	0.036±0.005	n.d	n.d.	0.4	n.d

^agiRI (growth inhibition resistance index) = IC₅₀ (PfW2)/IC₅₀ (Pf3D7). ^bcRI (cytotoxic resistance index) = LD₅₀ (PfDd2)/LD₅₀ (Pf3D7); n.d. = not determined.

between the aromatic groups of the β -hematin. Additionally, CQ may establish dipole–dipole interactions between the chlorine atom at C7 and the hydrogen atom of a methyl group of heme, and between the quinoline nitrogen atom and the hydrogen atom of vinyl groups of heme within the crevice. CQ may also bind to the Hz nucleation face {100} via electrostatic interactions between the side-chain amine and heme propionic acid groups exposed on that crystal surface and form additional hydrophobic interactions between the quinoline ring and methyl or vinyl C–H substituents of heme.

In recent years we have been involved in the design of new antimalarials based on the natural indoloquinoline alkaloid cryptolepine (**1a**, Chart 1).¹⁷ C-11 cryptolepine derivatives showed improved in vitro cytostatic activity and parasite selectivity compared to mammalian cells, but their mechanism of action was probably due to binding to both heme and DNA.^{17b} In addition, the most promising compound (**1b**) was only as active as the parent compound **1a** in a rodent malaria model, showing modest antimalarial efficacy when administered orally and high toxicity when administered ip at 50 mg/kg.¹⁸ To optimize the indolo[3,2-*b*]quinoline derivatives **1**, we focused on understanding the chemical features leading to Hz binding and increased inhibition of Hz formation. On the basis of the crystal structure of β -hematin and theoretical crystal growth,^{13a,b} isomers **2** and **3** (Chart 1) were designed to accumulate inside the DV and to bind to different Hz crystal faces. Our preliminary studies¹⁹ showed that interactions of bis-alkylamine indolo[3,2-*b*]quinoline derivatives **2** and **3** with hematin monomer could not explain per se the different growth inhibition effects observed against intraerythrocytic parasites, maybe reflecting the nonphysiologic conditions of the in vitro heme binding assays or because Hz ligands targeting different crystal faces can induce different antimalarial effects. To further address this late hypothesis, new compounds with increased chemical diversity (**2a–k** and **3a–k**; Scheme 1) were synthesized, and the in vitro cytostatic (IC_{50}) and cytotoxic (LD_{50}) activities against asexual intraerythrocytic forms of drug-resistant and sensitive strains of *P. falciparum* were assessed. Determinations of structure–activity relationships, cytostatic and cytotoxic stage specificities, effects on parasite morphology, correlations between IC_{50} s and LD_{50} s with hematin association constants, inhibition of β -hematin crystallization, and calculated vacuolar accumulation ratios (based on octanol/water distribution coefficients at pH 7.4 and 5.2) revealed the structural requirements to design new drugs targeting Hz. The specificities of compounds for parasites and heme/hemozoin targets were also assessed by comparing growth inhibition and DNA binding affinities in *Plasmodium* and human cells.

■ RESULTS AND DISCUSSION

Synthesis. Bis-alkylamine indolo[3,2-*b*]quinolines **2a–k** and **3a–k** were synthesized via quindolones **7** (indolo[3,2-*b*]quinolin-11-ones), as depicted in Scheme 1 and previously reported by us.¹⁹ Briefly, compounds **7a–h** were obtained from anthranilic acids **4a,b** after reaction with bromoacetyl bromide to afford **5a,b**, which were then converted to the corresponding 2-(2-(phenylamino)acetyl)benzoic acids **6a–h** by reaction with the appropriate aniline. Polyphosphoric acid (PPA) promoted bicyclization of **6a–h**, affording the corresponding quindolones **7a–h**. Finally, reflux of **7a–h** with 4 equiv of a chloroalkylamine in dry acetone and in the presence of Na_2CO_3 and NaI afforded mainly the bis-alkylamine derivatives **2a–k** and **3a–k**, which were then separated by preparative TLC on alumina. In

most cases, yields of isolated bis-alkylamine compounds ranged from 20% to 35%, and the formation in low yields (<10%) of O11-monoalkylated derivatives was also identified.¹⁹ Structures of **2a–k** and **3a–k** were completely elucidated by bidimensional ¹H and ¹³C heterocorrelation experiments (HMQC and HMBC). ¹³C NMR spectra of **3a–k** showed instead of the carbonyl carbon of the starting material resonating at 167 ppm, characteristic phenoxy carbon signals at ~145 ppm (C11) and typical ether carbon signals (~75 ppm) correlating in the HMQC with one deshielded triplet ¹H signal at ~4.3 ppm. The positions of *N*-alkylamine side chains of target compounds **2** and **3** were assigned on the basis of HMBC ¹H–¹³C correlations between CH₂ protons of side chains and quaternary carbons of the indoloquinoline aromatic structure and confirmed by nuclear Overhauser effect (NOE) experiments (Figure S1, Supporting Information).

Cytostatic Activity. Compounds of series **2** and **3** with purity $\geq 95\%$ were evaluated for their growth inhibition activity against erythrocytic stages of two strains of *P. falciparum*, the CQ-resistant W2 and the CQ-sensitive 3D7. Bis-alkylamine indolo[3,2-*b*]quinolines **2** and **3** showed a wide range of cytostatic activities, varying from highly active ($IC_{50} = 25$ nM; **3i** against W2) to poorly active ($IC_{50} = 2.5$ μ M, **2a** against 3D7). No cross-resistance with CQ was observed, as growth inhibition resistance indices (giRI), the ratio between the IC_{50} s for W2 and 3D7, were <1 (Table 1) or in the range 0.5–2 if determined by the ratio between the IC_{50} s for Dd2 and 3D7 (Table S1; Supporting Information).

Structure–activity relationship (SAR) analyses were performed for each series of compounds. N5,N10-Bis-alkylamine indolo[3,2-*b*]quinolines **2a–k** showed potent growth inhibition activity against strain W2 (IC_{50} s from 153 nM (**2i**) to 702 nM (**2a**)). The effect of side-chain length on activity was analyzed by comparing **2a** with **2c**, and **2b** with **2d**. Compounds with propyl side chains were more active than those with shorter ethyl side chains, although in the case of **2d** improved activity might have also been due to increased size of the terminal cyclic amine. This improvement in activity may reflect differences in compound binding to Hz crystal and/or lipophilicity. Introduction of a conformational constraint at the side-chain amine group increased activity (**2b** vs **2a**, and **2d** vs **2c**). Thus, growth inhibition activity was not exclusively dependent on lipophilicity, as **2b** is less lipophilic than **2a** (Table S2, Supporting Information). Compound flexibility has been shown to correlate negatively with drug permeation through membranes.²⁰ Therefore, the observation that **2b** was more active than **2a** most likely reflects increased membrane permeability and drug concentration at the target.

The effects of different substituents at positions 3 and 7 of the indolo[3,2-*b*]quinoline skeleton on parasite growth were also evaluated. Comparing the IC_{50} values for **2a**, **2e**, and **2h**, we can conclude that a chlorine atom at either position increased activity and that 3-Cl is preferred over 7-Cl substitution. Additionally, no significant differences were found between IC_{50} values for **2e**, **2f**, and **2g**, indicating that position 7 tolerates electron-withdrawing/X-bond donor/H-bond acceptor substituents including a chlorine atom (**2e**), electron-donating/H-bond acceptor substituents such as a methoxy group (**2f**), or small lipophilic groups such as a methyl group (**2g**). When a chlorine atom is at C3, another chlorine atom at C7 (**2i**) increased activity, but neither a methoxy group (**2j**) nor a lipophilic methyl group (**2k**) affected

Table 2. Cytotoxicity (IC₅₀) of 2 and 3 against the Human Hepatoma Cell Line HepG2 and Selectivity Indices for CQ-Resistant *P. falciparum* Strain W2 (SI_{res}) and CQ-Sensitive Strain 3D7 (SI_{sen})

compd	HepG2 IC ₅₀ (μM) ± SD	SI _{res} ^a	SI _{sen} ^b	compd	HepG2 IC ₅₀ (μM) ± SD	SI _{res} ^a	SI _{sen} ^b
2a	2.3 ± 0.1	3	1	3a	3.3 ± 0.3	6	3
2b	3.3 ± 0.2	8	3	3b	3.3 ± 0.4	7	3
2c	4.2 ± 1.1	12	3	3d	15.8 ± 0.9	144	35
2d	3.4 ± 0.1	20	7	3e	19.1 ± 0.7	102	62
2e	4.8 ± 0.4	12	5	3h	10.0 ± 0.8	99	29
2f	5.1 ± 0.7	12	3	3i	5.3 ± 0.2	212	34
2g	3.5 ± 0.1	9	3	3j	3.1 ± 0.5	23	8.3
2h	5.7 ± 0.8	22	8	3k	11.0 ± 2.5	63	45
2i	14.5 ± 1.4	95	35				
2j	2.4 ± 0.3	12	3				
2k	3.7 ± 0.2	14	4				

^aSI_{res} = IC₅₀ HepG2/IC₅₀ *Pf*W2. ^bSI_{sen} = IC₅₀ HepG2/IC₅₀ *Pf*3D7.

growth inhibition activity against the W2 and 3D7 strains, as IC₅₀ values for 2k and 2j were similar to that of 2h (7-H).

The N10,O11-bis-alkylamine indolo[3,2-*b*]quinoline derivatives 3a,b,d,e,h–k also showed potent parasite inhibition, with IC₅₀ values ranging from 25 nM (3i) to 533 nM (3a) against the W2 strain and from 156 nM (3i) to 1.27 μM (3a) against the 3D7 strain. In this series, an increase in side-chain length from ethyl to propyl also increased antiparasmodial activity (3d vs 3b), but in contrast with series 2, introduction of conformational constraint at the side-chain terminus had no clear effect on activity (3a and 3b were equally active; *P* > 0.05). Considering all chemical variations in C3 and C7 studied, the presence of chlorine atoms had the most significant impact on activity. The growth inhibition activity trend followed that observed for series 2, that is 3,7-di-Cl (3i) > 3-Cl (3h) ≥ 7-Cl (3e). Comparing with 3a, introduction of a chlorine atom at C7 (3e) increased activity from 3- (W2) to 4-fold (3D7), whereas a chlorine atom at C3 (3h) increased activity from 4- (3D7) to 5-fold (W2). Remarkably, compound 3i, with two chlorine atoms, had an increase in potency of 20-fold for W2. Taken together, chlorine atoms at positions 3 and/or 7 seem to be beneficial to activity, in line with SAR studies that have demonstrated the importance of a chlorine atom at C7 of CQ in antiparasmodial activity,²¹ inhibition of β-hematin,^{7b} or binding to the Hz crystal face {001}.¹⁶

The effect of the alkylamine side-chain substitution pattern on growth inhibition was also analyzed by comparing relative sensitivities of the two *P. falciparum* strains for each pair of isomers (e.g., 2a vs 3a, 2b vs 3b, etc.). In general, N10,O11-bis-alkylamine derivatives (series 3) were more active than the corresponding N5,N10-bis-alkylamine isomers (series 2), particularly for derivatives with chlorine substitutions (3e, 3h, and 3i vs 2e, 2h, and 2i).

Cytocidal Activity. To further evaluate the antiparasmodial activity of 2 and 3, eight compounds were selected on the basis of previous SAR and tested for their effects on asynchronous cultures of *P. falciparum* 3D7 and Dd2 (CQ resistant) strains, using the methodology previously reported by Roepe and co-workers.³ Concentrations killing 50% of parasites after a 6 h exposure (LD₅₀) are presented in Table 1 together with cytotoxic resistance indices (cRI, the ratio between the LD₅₀ against Dd2 and that against 3D7). As observed for cytostatic activity, tested compounds showed cytotoxic activities varying from very active (LD₅₀ = 156 nM; 3i against 3D7) to poorly active (LD₅₀ = 2.34 μM; 2a against Dd2) or inactive (LD₅₀ > 10 μM; 2a and 3b against 3D7) and cytotoxic resistance indices

(cRI) ≤ 1. In our assay, CQ showed LD₅₀ values and cRI comparable with values previously reported for *P. falciparum* HB3 and Dd2 strains.³ Although cytostatic activities reported in Table 1 were determined using a method different from that used to determine cytotoxic activities, results from the two methods are comparable (see Table S1; Supporting Information). Comparison of IC₅₀ with LD₅₀ values for 3D7 indicates that series 2 and 3 cytotoxic potency was 1.5-fold (2i and 3i) to 30-fold (3e) lower than growth inhibition potency. Structure–cytotoxic relationships follow the same general trend previously observed, that is, cytotoxic activity increased with conformational constraint at the side-chain amine group (2b is more active than 2a), with increasing lipophilicity (Figure S2A, Supporting Information), and with chlorine substitution, following the trend 3,7-di-Cl (3i) > 3-Cl (3h) > 7-Cl (3e). However, it must be noted that these observations can be biased by the fact that compounds tested for cytotoxic activity were selected based on SAR for cytostatic activity.

Cytotoxicity to Human Cells and DNA Binding. The *in vitro* cytotoxicity of compounds of series 2 and 3 was determined by assessing the viability of HepG2 A16 human hepatic cells after 48 h exposure to the compounds. Concentrations inhibiting cell viability by 50% (IC₅₀) ranged from 2.3 μM (2a and 2j) to 19.1 μM (3e) (Table 2), with no particular relationship between cytotoxicity and chemical variation or lipophilicity (Figure S3, Supporting Information). The best selectivity index was 212 calculated for 3i, the most active compound against the W2 strain.

DNA was previously shown to be a cellular target of indolo[3,2-*b*]quinoline derivatives 1,^{17b} which might explain the toxicity of these compounds.¹⁸ The strength of binding to double stranded (ds) DNA of series 2 and 3 was assessed by a fluorescence resonance energy transfer (FRET) melting assay.²² The increase in the melting temperatures of tagged self-complementary hairpin oligonucleotides induced by different concentrations of compounds 1b, 2b,d,k, and 3b,d,k is presented in Figure 1. The small differences in ds-DNA melting temperature (Δ*T*_m) induced by compounds 2b,d,k and compounds 3b,d,k at all concentrations tested (0.5 to 5 μM) indicate that these compounds are poor ligands of ds-DNA, contrary to the result observed for 1b.

Effects on Intraerythrocytic *P. falciparum* Development and Morphology. To study the effects of the most active compounds of each series on parasite morphology, synchronized ring-stage cultures of *P. falciparum* 3D7 were treated for 24 h with serial dilutions of 2i or 3i, and the

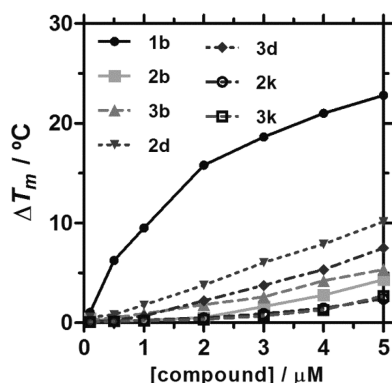


Figure 1. Binding of compounds **1b**, **2b,d,k**, and **3b,d,k**, at increasing concentrations, to double stranded DNA (self-complementary hairpin oligonucleotide), expressed as ΔT_m ($^{\circ}\text{C}$), measured by a fluorescence resonance energy transfer (FRET) melting assay.

morphologies of Giemsa-stained parasites were compared with those of parasites treated with CQ and MQ and with untreated controls (Figure 2). Control parasites developed from ring to

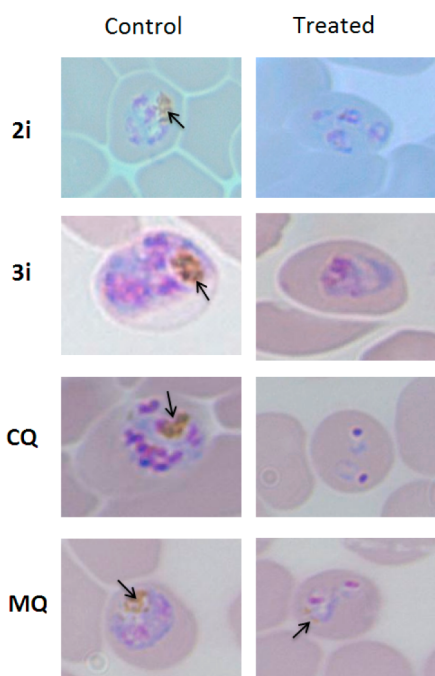


Figure 2. Giemsa-stained smears of *P. falciparum* (3D7)-infected erythrocytes treated with IC_{50} concentrations of **2i**, **3i**, CQ, and MQ for 24 h, beginning at the ring stage. Arrows indicate hemozoin inside parasites. Nuclei are stained pink and cytosol blue.

late-trophozoite/early schizont stage parasites, with Hz evident and typical morphological organization of the nuclei and cytoplasm. In parasites treated with CQ (IC_{50} concentration determined by light microscopy after 24 h incubation; Figure S4, Supporting Information), the majority of the parasites remained at the ring stage, without any visible Hz, consistent with prior observations²³ and suggesting that CQ delayed parasite development and inhibited Hz formation.^{24,9b} Parasites treated with MQ (IC_{50} concentration) developed to early trophozoites, with some accumulation of hemozoin, though with cytoplasmic vacuolization, also consistent with previous observations.^{25,23b,26} Similarly, parasites treated with com-

pounds **2i** and **3i** showed a marked developmental delay, exhibiting an early trophozoite-like appearance but lacking large DVs containing Hz crystals. This effect was more evident in the case of parasites treated with **3i**.

At higher doses a pronounced morphology arrest was seen for the four compounds (**2i**, **3i**, CQ, and MQ). Giemsa-stained smears revealed abundant shrunken parasites with pyknotic features (data not shown) as previously observed by others for CQ and MQ.^{25,27} In general, when compared to CQ and MQ, **2i** and **3i** induced similar parasite developmental impairment and morphological alterations, which may suggest a common mechanism of action, although additional studies are required to confirm this hypothesis.

Intraerythrocytic Stage Specificity. To study the developmental stage during which **3i** exerts its growth inhibition effects, *P. falciparum* 3D7 cultures were synchronized and **3i** at 33.5 nM ($\sim \text{IC}_{99}$ determined by light microscopy after 24 h incubation with synchronized ring stage 3D7 cultures; Figure S4, Supporting Information) was added to the culture medium at different parasite developmental stages. Parasites were grown in the absence or presence of **3i** until they had progressed to the subsequent ring stage (48 h for rings, 24 h for trophozoites, and 8 h for schizonts). The number of daughter rings following treatment was then estimated from Giemsa-stained smears by light microscopy. In the absence of **3i**, parasites displayed normal progression from rings to trophozoites, trophozoites to schizonts, and schizonts to rings (Figure 3). Treatment with **3i** during the ring or trophozoite stages resulted in a virtually complete inhibition of development, whereas treatment during the schizont stage only partially blocked parasite progression to daughter rings, reducing the number of rings in comparison to untreated parasites by $79.3 \pm 5.3\%$. Similarly, CQ, MQ, other 4-aminoquinolines, and amino alcohols were shown to almost completely inhibit parasite replication when added to rings and trophozoites but only to partially inhibit the development of mature blood stage parasites.²⁶

We also studied cytotoxic specificity and rate of action of **2** and **3** by incubating compounds with rings, trophozoites, or schizonts for 2 or 6 h (Figure 4 and Tables S3 and S4, Supporting Information). Indoloquinolines **2** and **3** showed general cytotoxic specificity for schizonts. CQ showed similar cytotoxic effects for all stages, although effects were slightly greater on schizonts after a 2 h incubation, in agreement with previous reports.²⁸ Interestingly, as catabolism of hemoglobin and Hz formation in schizonts is believed to be almost nonexistent,^{9a,29} the cytotoxic mechanism of action of bis-alkylamine-indoloquinolines in schizonts must be other than inhibition of Hz formation, in line with previous observations for CQ.³⁰

Binding to Hematin and β -Hematin Inhibition. The data described above, particularly the observation of early trophozoites without visible Hz after incubation of rings with **3i** and **2i** for 24 h, suggest that cytostatic antiparasitic activity of indolo[3,2-*b*]quinolines **2** and **3** may be due to inhibition of Hz biocrystallization. This prompted us to study the influence of alkylamine substitution pattern (**2a,d,h,i** vs **3a,d,h,i**) and chlorine substitution (**2a** vs **2h,i** or **3a** vs **3h,i**) on binding to hematin and on the capacity to inhibit the formation of β -hematin crystal in acidic media.

The equilibrium binding constants (K_{ass}) of compounds with hematin monomer were determined by UV–visible titration in pH 5.5 buffer containing 40% DMSO v/v to minimize

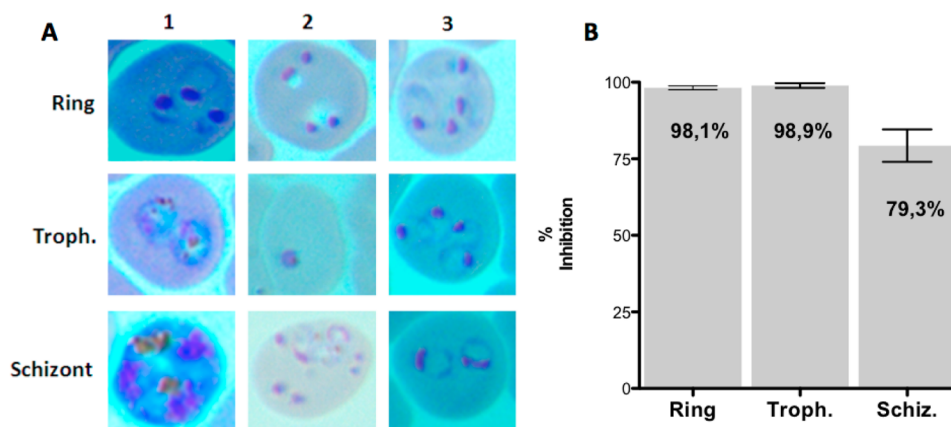


Figure 3. Stage specificity of growth inhibition by 3i. Highly synchronized *P. falciparum* 3D7 cultures were treated with 3i (33.5 nM) until they had progressed to the subsequent ring stage. A. Photomicrographs of treated and untreated parasites. B. Inhibition of formation of rings in the subsequent life cycle by incubation of 3i with different stages of parasites. Ring, ring stage; Troph., trophozoite stage; Schiz., schizont stage; 1, before treatment (0 h); 2, after treatment with 3i; 3, untreated control corresponding to the end of treatment.

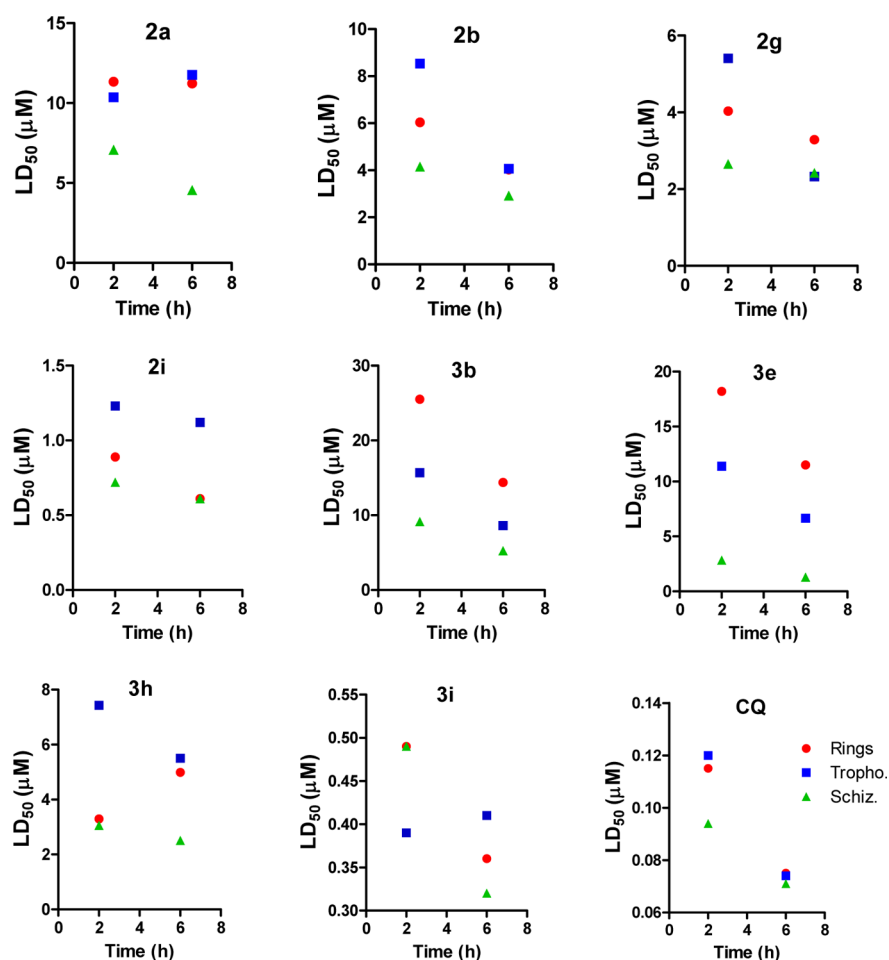


Figure 4. Cytocidal activity of compounds against *P. falciparum* 3D7-synchronized cultures of rings (red circles), trophozoites (blue squares), and schizonts (green triangles) after 2 and 6 h incubations.

porphyrin aggregation and dimer formation³¹ (Table 3; Figure S5, Supporting Information). A 1:1 binding stoichiometry was determined using the continuous variation technique (Job's plot),³² changing the hematin molar ratio and maintaining the sum of the concentrations of the ligand and hematin constant at 10 μM (Figure S6, Supporting Information). The determined K_{ass} of CQ in our assay ($0.85 \times 10^5 \text{ M}^{-1}$) was in

good agreement with that previously reported log K at pH = 4.97.³³ Inspection of Table 3 shows a general binding affinity trend of 3i > 2i > 2a, 2h, 3a, 3h, CQ, which indicates that bis-alkylamine indolo[3,2-*b*]quinoline derivatives, as well as CQ, have appropriate structural features to bind to hematin. Although the assay is performed in nonphysiological conditions, these results suggest that alkylamine substitution

Table 3. Association Constants (K_{ass}) of Compounds to Hematin and Inhibition of β -Hematin Crystal Formation in an Acetate Buffer by Compounds at 4 mM

compd	hematin $K_{\text{ass}} \pm \text{SD}$ ($\times 10^5 \text{ M}^{-1}$)	β -hematin inhibition ^a
2a	0.74 \pm 0.06	+
2d	n.d.	+
2h	0.76 \pm 0.06	+
2i	1.15 \pm 0.08	++
3a	0.80 \pm 0.10	+
3d	n.d.	+
3h	0.79 \pm 0.05	++
3i	1.4 \pm 0.02	+
CQ	0.85 \pm 0.05	+++
MQ	n.d.	–

^aInhibition of β -hematin formation by compounds at 4 mM (2:1 drug:hematin ratio) is expressed as – for <25%, + for \geq 25% and <50%, ++ for \geq 50% and <75%, +++ for \geq 75%; n.d., not determined.

pattern and 3,7-dichlorine substitution modulate binding affinity to hematin (3i has higher K_{ass} than 2i), in line with observed SAR.

As recently reviewed by Gorka et al.,¹⁰ several in vitro β -hematin inhibition assays using different experimental conditions (pH, ionic strength, temperature, catalysts, and work-up procedures) have been developed in the past years. However, as all these parameters, including organellar volume, will affect Hz formation and therefore inhibition of Hz by drugs, extrapolation of results from these in vitro assays to the physiologic situation must be made with caution. In this study, the ability of compounds 2a,d,h,i and 3a,d,h,i to inhibit β -hematin crystallization was assessed by the microtest previously reported by Basilico et al.³⁴ with some modifications. With this method, β -hematin crystals formed from hemin in acetate buffer (pH = 3), although produced in nonphysiologic conditions, were shown to be similar to natural Hz in shape, size,³⁵ and composition.^{34,36} For CQ, an IC_{50} of 0.85 equiv of hematin was determined from the dose-dependent inhibition curve (Figure S7, Supporting Information), in agreement with values previously reported.^{34,36} However, compounds of series 2 and 3, as well MQ, failed to produce a dose-dependent curve at the concentrations tested (4 mM to 0.5 mM) due to solubility limitations. Thus, we compared the percentage of β -hematin inhibition caused by compounds at 4 mM (2:1 drug:hematin ratio) with that of CQ. The semiquantitative results (Table 3) showed that, under the conditions of the assay, bis-alkylamine indolo[3,2-*b*]quinolines 2 and 3 were weaker inhibitors of β -hematin crystallization compared to CQ but better inhibitors than MQ. However, β -hematin inhibition data did not correlate with K_{ass} of compounds to hematin, maybe due to low precision of the method (SD up to 15%) or, most likely, because β -hematin inhibition by compounds is dependent not only on their binding affinities to hematin but also on compound-induced shifts of equilibria between β -hematin and other precrystalline forms such as μ -oxo-dimer or “head-to-tail” dimer. Interestingly, a correlation between antiparasitic activity (IC_{50}) and β -hematin inhibition by alkylamine derivatives of regioisomeric indolo[2,3-*b*]quinolines was recently reported.³⁷

Taken together, results from these two assays indicate that both series 2 and 3 have the structural features to bind to hematin and inhibit the formation of hemozoin in an acidic environment.

Vacuolar Accumulation Ratio (VAR) and Lipid Accumulation Ratio (LAR). Inhibition of Hz biocrystallization in ring and trophozoite stages³⁸ depends on drug concentration inside the parasite DV, where it can target hematin monomer or dimer soluble forms^{12a,b,11c} and Hz crystal.^{6a} Additionally, the capacity of a drug to accumulate in lipid phases may also be important to target Hz nucleation, because it has been shown to occur at the lipid–aqueous interface,³⁹ possibly mediated by lipid droplets inside the DV⁴⁰ or by an acylglycerol lipid film adsorbed to the inner leaflet of the DV membrane.^{6a}

In a simple model, the accumulation of an ionizable drug in a biological compartment is dependent on its distribution between lipid and aqueous phases at a given pH ($\log D_{\text{pH}}$), assuming that no particular transport mechanism is involved. The accumulation ratios between parasite cytosol (pH = 7.4) and vacuolar water at pH 5.2 (VAR),⁴¹ and lipid accumulation ratios (LAR)⁴¹ for selected compounds 2 and 3, are presented in Table 4 and were calculated based on experimental

Table 4. Distribution Coefficients of Compounds at pH 7.4 and 5.2 and Corresponding Vacuolar Accumulation Ratios (VAR) and Lipid Accumulation Ratios (LAR)

compd	$\log D_{7.4} \pm \text{SEM}$	$\log D_{5.2} \pm \text{SEM}$	VAR	LAR
2a	1.7 \pm 0.09	0.27 \pm 0.06	29	54
2b	1.3 \pm 0.04	0.33 \pm 0.05	10	22
2g	2.2 \pm 0.01	0.83 \pm 0.04	22	147
2i	3.01 ^a	1.6 \pm 0.02	27	1023
3b	1.4 \pm 0.03	0.27 \pm 0.03	14	25
3e	2.5 ^a	1.1 \pm 0.04	22	295
3h	2.5 ^a	1.1 \pm 0.02	22	295
3i	3.1 ^a	1.4 \pm 0.02	54	1230
CQ	–0.33 \pm 0.05	–1.2 \pm 0.1	7	0.5
	0.85 ^b	–1.2 ^b	112 ^b	7

^aValues determined from equation $\log D_{7.4} = 1.0581 \times \text{ClogP} - 3.4452$; $R^2 = 0.997$. ^bValues from Dubar et al.⁴²

distribution coefficients at pH 7.4 ($\log D_{7.4}$) and 5.2 ($\log D_{5.2}$). The exceptions were 2i, 3e,h,i as the high lipophilicity of these compounds precluded their quantification in the aqueous phase, even using an aqueous:lipid volume ratio of 10:1. Thus, $\log D_{7.4}$ for compounds 2i, 3e,h,i were calculated from respective ClogP values (Table S2, Supporting Information) applying the linear regression equation of $\log D_{7.4}$ as a function of ClogP of related compounds 2a,b,g and 3b (Figure S8, Supporting Information).

Compounds of series 2 and 3 were more lipophilic than CQ at both pHs, with $\log D_{7.4}$ varying between 1.3 (2b) and 3.1 (3i) and $\log D_{5.2}$ varying between 0.27 (2a/ 3b) and 1.6 (2i). The $\log D_{5.2}$ obtained for CQ was very similar to that previously reported⁴² and obtained using the same *n*-octanol–water ratio (1:1) and CQ concentration (40 $\mu\text{g/mL}$), whereas $\log D_{7.4}$ determined under the same conditions as $\log D_{5.2}$ was much lower than that previously reported,⁴² probably due to the use of a different *n*-octanol:phosphate buffer ratio. However, on the basis of $\log D_{7.4}$ and $\log D_{5.2}$ and independent of the experimental method used, CQ is predicted to accumulate in the DV 15 times more than in lipid media (LAR). In contrast, compounds of series 2 and 3 are expected to accumulate to higher concentrations in lipid membranes or lipid vesicles inside the DV compared to DV aqueous medium, as the calculated LAR is always higher than the corresponding calculated VAR.

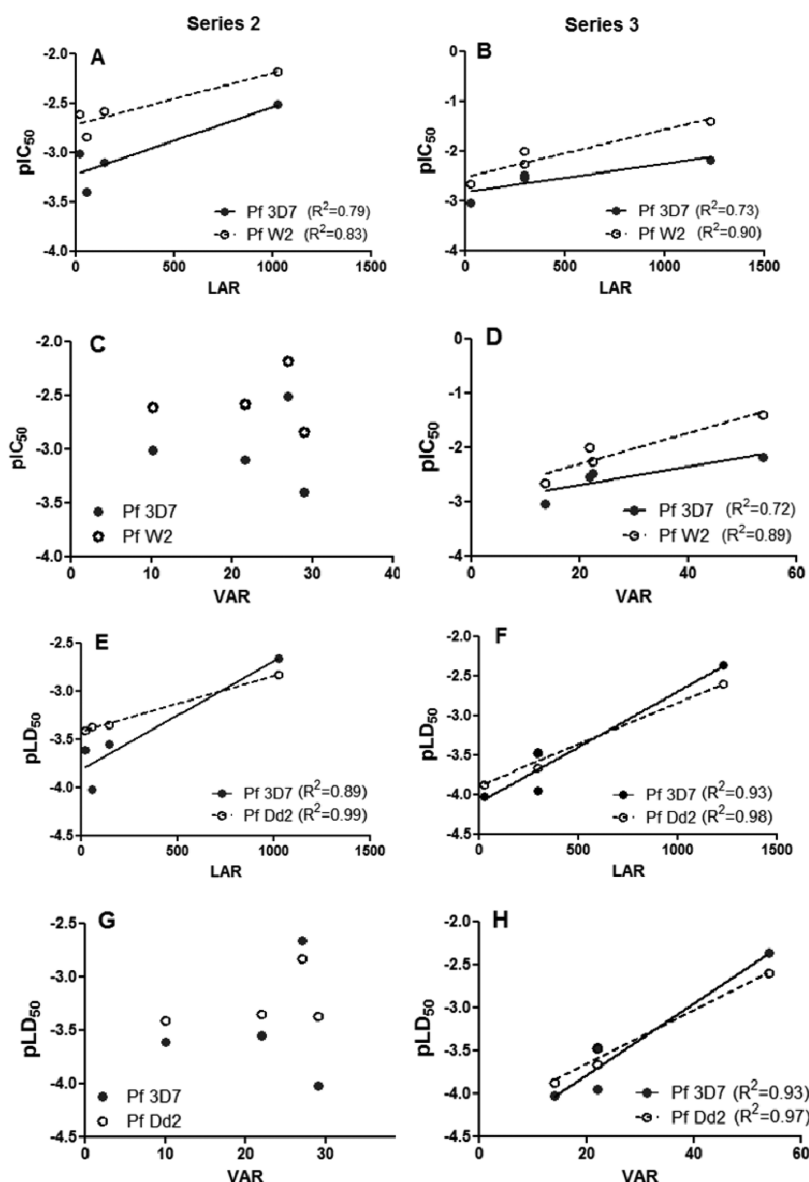


Figure 5. Correlation between antiparasmodial activities of compounds **2a,b,g,i** (left column) and **3b,e,h,i** (right column) for *P. falciparum* (3D7, W2, and Dd2 strains) and compound calculated lipid accumulation ratios (LAR; plots A, B, E, F) or calculated vacuolar accumulation ratios (VAR; plots C, D, G, H). Plots A–D refer to cytostatic activity (pIC_{50} , values in Table 1) and plots E–H refer to cytotoxic activity (pLD_{50}) against asynchronous intraerythrocytic parasite cultures after 6 h drug exposures (values in Table 1).

Inspection of Table 4 shows that the calculated VAR and LAR values for **2b** and **2i** compare to those of **3b** and **3i**, suggesting that pairs of compounds in isomeric series 2 and 3 are able to accumulate to the same extent inside the DV as well as in membranes or lipid particles. However, when VAR and LAR were correlated with antiparasmodial activity, significant differences were seen between the two series of compounds (Figure 5). These data suggest that antiparasmodial activity (cytostatic and cytotoxic) of isomers 3 depends on the capacity to concentrate at membranes (LAR) and inside an acidic compartment (VAR), whereas antiparasmodial activity of **2** depends only on the LAR. Although correlations of pIC_{50} with LAR are not statistically significant for a 95% confidence interval, maybe due to reduced number of compounds of each series used, plots of compound activity (pIC_{50} and pLD_{50}) versus ClogP (Figure S2, A and B; Supporting Information) indicate that antiparasmodial activity increases with lipophilicity

for both series. Several studies with CQ-related antimalarials have shown that lipophilicity correlates negatively with growth inhibition resistance index (giRI),^{41,43} and this observation has been explained by the capacity of more lipophilic compounds to act as PfCRT protein ligands.^{41,43a} However, in the case of series 2 and 3, both giRI and cRI do not correlate with lipophilicity (Figure S2, C and D; Supporting Information), possibly reflecting the noninterference of these compounds in the mechanisms of CQ-resistance in the W2 and Dd2 strains.

Cytotoxic activities of isomers 3 for rings, trophozoites, and schizonts also correlated with VAR (Figure 6) but not those of isomers 2 (plots not shown), suggesting another target inside the DV for series 3, because in late schizonts hemoglobin catabolism and Hz formation no longer occur.

Proposed Binding Mode of Series 2 and 3 to Hemozoin Crystal and Implications for Intraerythrocytic Antiparasmodial Activity. The in vitro studies indicate that

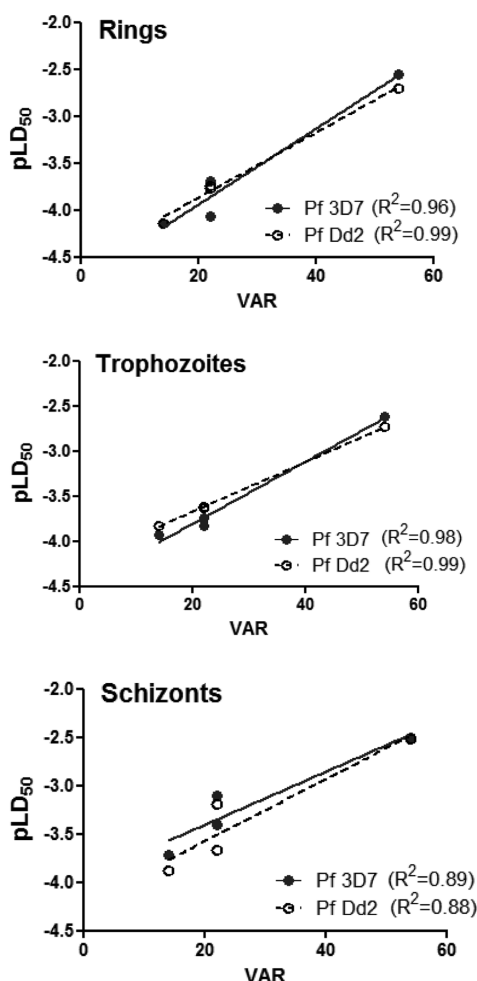


Figure 6. Correlation between stage specific cytotoxic activities (pLD₅₀) of compounds **3b,e,h,i** (6 h drug exposure; values in Tables S3 and S4) and calculated vacuole accumulation ratio (VAR).

series **2** and **3** have the structural features and physicochemical properties required to accumulate in DV and inhibit hemozoin formation by hemozoin sequestration. However, this mechanism explains neither the schizontocidal activity observed for both series nor the absence of correlation between antiparasitic activity (IC₅₀ and LD₅₀) and calculated ability of series **2** to accumulate in an acidic compartment (VAR).

Antimalarial activity of quinoline containing drugs has long been accepted to be due to inhibition of Hz formation inside the DV, although the exact mechanism is still not fully understood, and neither is the mechanism of hemozoin formation inside parasite DV. Several studies have shown that nucleation of Hz in cell-free systems (β -hematin) occurs at lipid–water interfaces^{40,39a,44} with biologically relevant half-life values.^{39a,b,45} In addition, recent studies applying several X-ray techniques suggest that Hz nucleation occurs at the DV inner membrane's bilayer, possibly catalyzed by mono- and diacyl lipids embodying the membrane inner leaflet, leading to the formation of a flat and well exposed Hz face {100},^{6a,46,47} whereas crystal growth has been proposed to occur within the aqueous phase.^{6a,13} This would explain the mechanism of Hz inhibition by hydrophilic antimalarials such as CQ, which has been proposed to occur primarily by adsorption of the molecule to the fast growing face {001}.^{16,13} This mechanism of Hz inhibition by CQ has recently been corroborated by

kinetic studies of β -hematin formation in biomimetic lipid–water emulsions.¹⁵ Taken together, it is reasonable to conclude that antiparasitic activity of compounds inhibiting Hz growth by adsorbance to the crystal face {001} depends on their capacity to accumulate in the DV aqueous medium (VAR) and on their binding affinities to that corrugated face. On the other hand, inhibition of Hz nucleation depends on compound binding affinities to the crystal face {100} and their accumulation in DV membranes (LAR). Thus, based on results present in Figures 5 and 6, we propose that cytostatic and cytotoxic activity of both series **2** and **3** are likely to be due, at least in part, to binding to Hz crystal face {100}, whereas compounds of series **3** may be also able to bind to the Hz crystal face {001} in DV aqueous medium, which would justify the general increased antiparasitic activity of series **3** compared to isomers **2**.

In analogy with the theoretical model of CQ binding to the Hz crystal face {001},^{13,16} the tetracyclic aromatic structure of compounds of series **3** may fit between the heme molecules of this crystal face, with both alkylamine side chains standing out of the crevice and being able to target the hemozoin carboxylate groups. Moreover, indoloquinoline N5 and chlorine at position 3 could establish additional interactions with, respectively, electron-deficient hydrogen atoms of vinyl and methyl groups of a heme molecule inside the crevice. Compounds of series **2** have a similar capacity as that of series **3** to accumulate in DV aqueous medium (Table 4), but the opposite location of their two side chains probably prevents the intercalation of the indoloquinoline structure within the crevice of the Hz crystal face {001}. Thus, their antiparasitic activity is independent of their accumulation in the DV (VAR). On the other hand, the Hz crystal nucleation face {100} exposes carboxylate groups distanced by 8 or 14.7 Å along the *c*- and *a*-axes, respectively,^{48,13a} which may be targeted by the amine groups of the two side chains of **2** and **3**, as calculated distances between amine groups are 7.3–10.6 Å (Figure S9, Supporting Information). Additionally, “T” type face-on-edge contact between the planar indoloquinoline nucleus and peripheral porphyrin C–H groups can strengthen binding to Hz, and additional interactions can be established between heme CH₃ and C=CH groups exposed on that crystal face and H-bond acceptors present in series **2**, such as C=O, Cl, OCH₃, and in **3** (Cl, O11-(CH₂)_n).

CONCLUSIONS

Hemozoin (Hz) is a heme detoxification product present in all forms of blood stage malaria parasites, and inhibition of its formation has long been accepted as the primary target of quinoline-containing antimalarials.⁷ Recent investigations of the Hz crystal structure,⁴⁸ theoretical drug–Hz interactions^{13b,16} and suggestions that the cytotoxic activity of quinoline-containing antimalarials may not be due to inhibition of hemozoin formation by hemozoin sequestration¹⁴ led us to design and synthesize two isomeric series of indolo[3,2-*b*]quinolines, N5,N10-bis-alkylamine derivatives **2a–k** and N10,O11-bis-alkylamine derivatives **3a–k**, aiming to explore the implications for antimalarial cytostatic and cytotoxic activities of targeting different Hz crystal faces. Both series were selective for malaria parasites (Table 2) and had decreased binding affinity to DNA compared to previous indoloquinoline derivatives **1** (Figure 1). Series **2** and **3** showed a wide range of cytostatic and cytotoxic activities (Table 1), allowing the establishment of important structure–activity relationships that

combined with stage specificity studies; effects on parasite morphology; and correlations of activities with association constants to hematin, inhibition of β -hematin crystallization, lipophilicity, and vacuolar accumulation ratios led us to conclude that the intraerythrocytic cytostatic antimalarial effects of **2** and **3** are maybe due to interactions with Hz crystals and consequent inhibition of Hz nucleation and crystal growth, although additional mechanisms of action cannot be excluded.

Overall, our results allow the following conclusions on the SAR and interactions of **2** and **3** with Hz: (1) both cytostatic and cytotoxic activities increase with increased lipophilicity (Figures 5 and S2), in agreement with increased accumulation of compounds in the DV inner membrane and in lipid bodies inside the DV, where they may inhibit Hz nucleation by binding to the Hz crystal face {100}; (2) the presence of two side chains on opposite sides of the tetracyclic indoloquinoline ring, such as in the case of N5,N10-bis-alkylamine isomers **2**, is detrimental for antiplasmodial activity, as this may prevent binding to the fast growing Hz crystal face {001}; (3) a chlorine atom at C3 increases antiplasmodial activity of both **2** and **3**; (4) introduction of a second chlorine atom at C7 (**2i** and **3i**) further increases antiplasmodial activity, in agreement with increased lipophilicity and observed increased binding affinity to hematin monomer (Table 3).

To the best of our knowledge, this is the first report on the use of β -hematin structure⁴⁸ to design novel antimalarial compounds targeting several chemical groups exposed on nucleation and fast-growing Hz crystal faces. Our findings, particularly the observed consistency of correlations between cytostatic or cytotoxic activities of **3**, but not of isomers **2**, and pH-dependent accumulation ratios (VAR), suggest that the two isomeric series may have different capacities to bind to Hz crystal face {001} and different mechanisms of cytotoxic potency. Moreover, we believe that SARs reported here will be relevant for the rational design of new and more active blood stage antimalarials targeting Hz. This strategy can also be applied to the design of drugs targeting other intraerythrocytic parasites, such as *Schistosoma* which cause a chronic illness in African countries, once their Hz crystal structures are elucidated.⁴⁹

EXPERIMENTAL SECTION

Chemistry. Chemicals were purchased from Sigma-Aldrich Chemical Co. Ltd., Spain, and used without further purification. All compounds were characterized by NMR spectroscopy, recorded on a Bruker Avance 400 spectrometer at 400 MHz (¹H NMR) and 100 MHz (¹³C) and using solvent as internal reference. Chemical shifts (δ) are expressed in ppm. Signal splitting patterns are described as singlet (s), doublet (d), triplet (t), quartet (q), quintet (quint), and multiplet (m), or combination thereof. Coupling constants (J) are given in hertz. The purity of compounds submitted to biological tests were in all cases $\geq 95\%$ as determined from elemental analysis C, H, and N analysis, carried out by the Unit Elemental Analysis, University of Santiago de Compostela, Spain, on a LECO model CHNS-932 elemental analyzer. Mass spectra were recorded using a Micromass Quattro Micro API, Waters. Mass spectra were obtained by direct infusion on "full scan" mode (m/z 60–800), and sample ionization was made in positive and negative electrospray ionization mode (ESI+ and ESI–). Reactions were monitored by thin-layer chromatography (TLC) using coated silica gel plates (Merck, aluminum sheets, silica gel 60 F254) or aluminum oxide matrix plates (Sigma-Aldrich, PET support, F254). Preparative thin layer chromatography (PTLC) was performed in aluminum oxide 60 F254 (VWR, 200 \times 200 mm glass support, F254).

General Procedure A. 2-(2-Bromoacetamido)benzoic Acid (5a**).** A solution of 2-aminobenzoic acid (10.0 g, 72.9 mmol) in DMF (30

mL) and 1,4-dioxane (30 mL) was cooled to 0 °C. Bromoacetyl bromide (8.0 mL, 91.7 mmol, 1.25 equiv) was added dropwise over a 20 min period, keeping the internal temperature between 0 °C and 5 °C. After the addition was complete, the ice bath was removed and stirring was continued overnight at room temperature. The reaction mixture was added to water (300 mL), and the light yellow precipitate which formed was filtered, washed with water until neutral pH, and then dried to give 18.1 g (96%) of **5a** as a white solid, mp 162–165 °C. ¹H NMR (400 MHz, DMSO) δ_H (ppm) 11.23 (s, NH), 8.06 (d, J = 8.4 Hz, 1H), 7.62 (dd, J = 7.9, 1.4 Hz, 1H), 7.24 (dd, J = 8.4, 7.3 Hz, 1H), 6.82 (dd, J = 7.9, 7.3 Hz, 1H), 3.87 (s, 2H). ¹³C NMR (100 MHz, DMSO) δ_C (ppm) 169.20, 165.04, 139.92, 134.06, 131.11, 123.45, 119.99, 117.06, 30.65. ESI-MS: [$M + H$]⁺ m/z 259.90.

2-(2-Bromoacetamido)-4-chlorobenzoic Acid (5b**).** Reaction of 2-amino-4-chlorobenzoic acid (10 g, 58.2 mmol) and bromoacetyl bromide (14.7 g, 6.3 mL, 72.8 mmol, 1.25 equiv) according to general procedure A, gave 17.1 g (99%) of **5b** as a light yellow solid, mp 166–168 °C. ¹H NMR (400 MHz, DMSO) δ_H (ppm) 11.73 (s, NH), 8.54 (d, J = 2.1 Hz, 1H), 7.98 (d, J = 8.6 Hz, 1H), 7.24 (dd, J = 8.6, 2.1 Hz, 1H), 4.28 (s, 2H). ¹³C NMR (100 MHz, DMSO) δ_C (ppm) 169.03, 165.92, 141.54, 138.95, 133.26, 123.73, 119.61, 115.91, 30.98.

General Procedure B. Synthesis of 2-[2-(Phenylamino)acetamido]benzoic Acid (6a**).** A solution of **5a** (15.0 g, 58.1 mmol) and aniline (19.0 mL, 203.4 mmol, 3.5 equiv) in DMF (30 mL) was heated at 120 °C for 18 h. After cooling, the reaction mixture was poured into ice–water (500 mL), and aqueous 5% KOH was added to solubilize the solid product and adjust the pH to 10. Then the mixture was washed with dichloromethane (3 \times 200 mL). The combined dichloromethane extracts were set aside and the aqueous layer was acidified to pH 3 with 5% HBr. The precipitate which formed was collected, washed with water, and then dried, yielding 11.0 g (70%) of **6a** as a white solid. ¹H NMR (400 MHz, DMSO) δ_H (ppm) 11.96 (s, NH), 8.61 (d, J = 8.7 Hz, 1H), 7.83 (d, J = 7.9 Hz, 1H), 7.47 (dd, J = 8.7, 8.0 Hz, 1H), 7.02 (dd, J = 8.0, 7.9 Hz, 1H), 6.98 (d, J = 7.3 Hz, 2H), 6.50 (d, J = 7.7 Hz, 1H), 6.48 (dd, J = 7.7, 7.3 Hz, 2H), 6.39 (s, NH), 3.73 (s, 2H). ¹³C NMR (100 MHz, CD₃OD) δ_C (ppm): 170.82, 169.01, 148.08, 140.52, 134.03, 131.08, 128.92, 122.60, 119.32, 116.98, 116.12, 112.36, 48.89. ESI-MS: [$M + H$]⁺ m/z 270.99.

2-[2-[(4-Chlorophenyl)amino]acetamido]benzoic Acid (6b**).** Reaction of **5a** (15 g, 58.1 mmol) with 4-chloroaniline (23.0 g, 180.1 mmol, 3.1 equiv) for 96 h according to general procedure B gave 3.90 g of **6b** (22%) as a slightly yellow solid. ¹H NMR (400 MHz, DMSO) δ_H (ppm) 11.97 (s, NH), 8.70 (d, J = 8.4 Hz, 1H), 7.94 (dd, J = 7.9, 1.5 Hz, 1H), 7.59 (ddd, J = 8.4, 7.9, 1.5 Hz, 1H), 7.17–7.10 (m, 3H), 6.71 (t, J = 5.5 Hz, NH), 6.59 (d, J = 8.9 Hz, 2H), 3.84 (d, J = 5.5 Hz, 2H). ¹³C NMR (100 MHz, DMSO) δ_C (ppm) 170.48, 169.18, 147.09, 140.57, 134.24, 131.21, 128.76, 122.80, 120.38, 119.44, 116.04, 113.86, 48.77. ESI-MS: [$M + H$]⁺ m/z 304.94.

2-[2-[(4-Methoxyphenyl)amino]acetamido]benzoic Acid (6c**).** Reaction of **5a** (15 g, 58.1 mmol) with *p*-anisidine (25.0 g, 203.4 mmol, 3.5 equiv) according to general procedure B gave 13.3 g of **6c** (76%) as a brown solid. ¹H NMR (400 MHz, DMSO) δ_H (ppm) 12.06 (s, NH), 8.72 (d, J = 8.5 Hz, 1H), 7.93 (dd, J = 8.0, 1.6 Hz, 1H), 7.58 (ddd, J = 8.5, 7.7, 1.6 Hz, 1H), 7.12 (ddd, J = 8.0, 7.7, 1.2 Hz, 1H), 6.73 (d, J = 8.9 Hz, 2H), 6.53 (d, J = 8.9 Hz, 2H), 3.76 (s, 2H), 3.62 (s, 3H). ¹³C NMR (100 MHz, DMSO) δ_C (ppm) 171.23, 169.01, 151.53, 142.25, 140.61, 134.13, 131.17, 122.66, 119.42, 116.15, 114.60, 113.44, 55.24, 49.80.

2-[2-(*p*-Tolylamino)acetamido]benzoic Acid (6d**).** Reaction of **5a** (15 g, 58.1 mmol) with *p*-toluidine (21.8 g, 203.4 mmol, 3.5 equiv) for 24 h according to general procedure B gave 8.42 g of **6d** (51%) as a brown solid. ¹H NMR (400 MHz, DMSO) δ_H (ppm) 12.04 (s, NH), 8.74 (d, J = 8.4 Hz, 1H), 7.94 (d, J = 7.8 Hz, 1H), 7.58 (dd, J = 8.4, 7.8 Hz, 1H), 7.12 (dd, J = 8.4, 7.6 Hz, 1H), 6.63 (d, J = 6.9 Hz, 2H), 6.50 (d, J = 7.9 Hz, 2H), 3.80 (s, 2H), 2.13 (s, 3H). ¹³C NMR (100 MHz, DMSO) δ_C (ppm) 171.14, 169.06, 145.91, 140.65, 134.18, 131.18, 129.47, 125.53, 122.67, 119.43, 116.064, 112.55, 49.34, 20.13.

4-Chloro-2-[2-(phenylamino)acetamido]benzoic Acid (6e**).** Reaction of **5b** (15 g, 51.3 mmol) with aniline (16.7 g, 16.3 mL, 179.6 mmol, 3.5 equiv) according to general procedure B gave 11.8 g of **6e**

(76%) as a white solid. ^1H NMR (400 MHz, DMSO) δ_{H} (ppm) 12.13 (s, NH), 8.83 (d, $J = 2.2$ Hz, 1H), 7.94 (d, $J = 8.6$ Hz, 1H), 7.21 (dd, $J = 8.6, 2.2$ Hz, 1H), 7.10 (dd, $J = 8.0, 7.4$ Hz, 2H), 6.63 (d, $J = 7.4$ Hz, 1H), 6.59 (d, $J = 8.0$ Hz, 2H), 3.86 (s, 2H). ^{13}C NMR (100 MHz, DMSO) δ_{C} (ppm) 171.96, 168.80, 148.46, 141.99, 139.03, 133.33, 129.45, 123.08, 119.16, 117.63, 115.16, 112.90, 49.36.

4-Chloro-2-[(4-chlorophenyl)amino]acetamido]benzoic Acid (6f). Reaction of **5b** (3.0 g, 10.2 mmol) and 4-chloroaniline (4.04 g, 3.34 mL, 31.7 mmol, 3 equiv) in DMF (10 mL) was heated at 120 °C for 48 h and then treated according to general procedure B to give 2.47 g (70%) of **6f** as a white solid. ^1H NMR (400 MHz, DMSO) δ_{H} (ppm) 12.07 (s, 1H), 8.81 (s, 1H), 7.95 (d, $J = 8.6$ Hz, 1H), 7.22 (dd, $J = 8.6, 2.2$ Hz, 1H), 7.13 (d, $J = 8.8$ Hz, 2H), 6.73 (s, 1H), 6.60 (d, $J = 8.9$ Hz, 2H), 3.88 (d, $J = 4.9$ Hz, 2H). ^{13}C NMR (100 MHz, DMSO) δ_{C} (ppm) 171.48, 168.87, 147.39, 141.94, 139.05, 133.35, 129.17, 123.15, 120.91, 119.17, 115.15, 114.31, 49.13. ESI-MS: $[\text{M} + \text{H}]^+ m/z$ 338.93.

4-Chloro-2-[(4-methoxyphenyl)amino]acetamido]benzoic Acid (6g). Reaction of **5b** (3.0 g, 10.25 mmol) and 4-methoxyaniline (3.79 g, 30.75 mmol, 3 equiv) in DMF (10 mL) was heated at 120 °C for 96 h and treated according to general procedure B to give 2.52 g (72%) of **6g** as a light brown solid. ^1H NMR (400 MHz, DMSO) δ_{H} (ppm) 12.16 (s, NH), 8.84 (d, $J = 2.2$ Hz, 1H), 7.94 (d, $J = 8.5$ Hz, 1H), 7.21 (dd, $J = 8.5, 2.2$ Hz, 1H), 6.73 (d, $J = 8.9$ Hz, 2H), 6.54 (d, $J = 8.9$ Hz, 2H), 3.79 (s, 2H), 3.62 (s, 3H). ^{13}C NMR (100 MHz, DMSO) δ_{C} (ppm) 172.25, 168.70, 152.03, 142.52, 141.99, 138.99, 133.32, 123.02, 119.15, 115.22, 115.02, 113.90, 55.63, 50.16.

4-Chloro-2-[(4-methylphenyl)amino]acetamido]benzoic Acid (6h). A solution of **5b** (4.0 g, 13.6 mmol) and 4-methylaniline (2.93 g, 27.3 mmol, 2 equiv) in DMF (15 mL) was heated at 120 °C for 48 h and treated according to general procedure B to give 3.68 g (83%) of **6h** as a light yellow solid. ^1H NMR (400 MHz, DMSO) δ_{H} (ppm) 12.13 (s, 1H), 8.83 (d, $J = 2.0$ Hz, 1H), 7.94 (d, $J = 8.5$ Hz, 1H), 7.21 (dd, $J = 8.5, 2.0$ Hz, 1H), 6.91 (d, $J = 8.3$ Hz, 2H), 6.49 (d, $J = 8.3$ Hz, 2H), 3.81 (s, 2H), 2.14 (s, 3H). ^{13}C NMR (100 MHz, DMSO) δ_{C} (ppm) 172.15, 168.74, 146.19, 142.00, 139.02, 133.32, 129.88, 126.05, 123.04, 119.14, 115.14, 112.96, 49.67, 20.53.

General procedure C. 5H-Indolo[3,2-b]quinolin-11(10H)-one (7a).^{17b} A mixture of **6a** (6.0 g, 21.5 mmol) and polyphosphoric acid (PPA, 160 g) was heated with mechanical stirring at 130 °C for 2 h. The reaction mixture was added to ice-water (500 mL), neutralized with saturated KOH solution, and then extracted with EtOAc (3 × 500 mL). The extract was washed with water and dried with brine and anhydrous Na_2SO_4 , and then the solvent was removed at reduced pressure. The product was recrystallized from EtOAc with diethyl ether:hexane (9:1) to give 3.47 g (67%) of **7a** as a light-brown solid. ^1H NMR (400 MHz, DMSO) δ_{H} (ppm) 12.81 (s, 1H), 11.69 (s, 1H), 8.35 (d, $J = 8.0$ Hz, 1H), 8.28 (d, $J = 8.0$ Hz, 1H), 7.81 (d, $J = 8.4$ Hz, 1H), 7.68 (dd, $J = 8.4, 7.5$ Hz, 1H), 7.50 (d, $J = 8.2, 1\text{H}$), 7.49 (dd, $J = 8.2, 7.4$ Hz, 1H), 7.28 (dd, $J = 8.0, 7.5$ Hz, 1H), 7.20 (dd, $J = 8.0, 7.4$ Hz, 1H). ^{13}C NMR (100 MHz, DMSO) δ_{C} (ppm) 167.77, 139.54, 139.05, 130.99, 129.44, 127.84, 125.57, 123.48, 123.24, 121.63, 120.87, 119.25, 118.28, 116.38, 112.98. ESI-MS: $[\text{M} + \text{H}]^+ m/z$ 235.01.

7-Chloro-5H-indolo[3,2-b]quinolin-11(10H)-one (7b). A mixture of **6b** (6.0 g, 19.7 mmol) and PPA (160 g) was treated according to general procedure C, giving 4.18 g (79%) of **7b** as a light-brown solid. ^1H NMR (400 MHz, DMSO) δ_{H} (ppm) 12.47 (s, NH), 11.92 (s, NH), 8.35 (d, $J = 8.1$ Hz, 1H), 8.25 (d, $J = 1.9$ Hz, 1H), 7.72–7.68 (m, 2H), 7.53 (d, $J = 8.7$ Hz, 1H), 7.47 (dd, $J = 8.7, 1.9$ Hz, 1H), 7.29 (dd, $J = 8.1, 7.7$ Hz, 1H). ^{13}C NMR (100 MHz, DMSO) δ_{C} (ppm) 167.67, 139.14, 136.90, 131.08, 128.06, 127.38, 125.27, 123.99, 123.06, 122.84, 120.74, 120.15, 117.87, 116.80, 114.37. ESI-MS: $[\text{M} + \text{H}]^+ m/z$ 268.94.

7-Methoxy-5H-indolo[3,2-b]quinolin-11(10H)-one (7c). A mixture of **6c** (6.0 g, 20.0 mmol) and PPA (160 g) was treated according to general procedure C, giving 1.214 g (23%) of **7c** as a dark brown solid. ^1H NMR (400 MHz, DMSO) δ_{H} (ppm) 12.38 (s, NH), 11.51 (s, NH), 8.34 (d, $J = 8.0$ Hz, 1H), 7.73–7.63 (m, 3H), 7.42 (d, $J = 9.0$ Hz, 1H), 7.27 (ddd, $J = 8.6, 7.5, 1.2$ Hz, 1H), 7.13 (dd, $J = 9.0, 2.5$ Hz, 1H), 3.86 (s, 3H). ^{13}C NMR (100 MHz, DMSO) δ_{C} (ppm) 167.46,

152.90, 139.04, 133.98, 130.66, 128.71, 125.24, 123.79, 122.65, 120.30, 118.41, 117.70, 115.67, 113.68, 101.38, 55.41. ESI-MS: $[\text{M} + \text{H}]^+ m/z$ 264.98.

7-Methyl-5H-indolo[3,2-b]quinolin-11(10H)-one (7d). A mixture of **6d** (6.0 g, 21.1 mmol) and PPA (160 g) was treated according to general procedure C, giving 0.587 g (11%) of **7d** as a light-brown solid. ^1H NMR (400 MHz, DMSO) δ_{H} (ppm) 12.40 (s, NH), 11.56 (s, NH), 8.34 (d, $J = 8.3$ Hz, 1H), 7.97 (s, 1H), 7.72 (d, $J = 8.3$ Hz, 1H), 7.67 (ddd, $J = 8.4, 7.5, 1.3$ Hz, 1H), 7.42 (d, $J = 8.5$ Hz, 1H), 7.31 (dd, $J = 8.5, 1.3$ Hz, 1H), 7.28 (ddd, $J = 8.4, 7.5, 1.3$ Hz, 1H), 2.48 (s, 3H). ^{13}C NMR (100 MHz, DMSO) δ_{C} (ppm) 167.35, 139.04, 137.14, 130.62, 129.24, 128.63, 127.61, 125.21, 123.24, 122.79, 120.43, 120.08, 117.79, 115.98, 112.45, 21.23. ESI-MS: $[\text{M} + \text{H}]^+ m/z$ 249.01.

3-Chloro-5H-indolo[3,2-b]quinolin-11(10H)-one (7e).^{17b} A mixture of **6e** (2.0 g, 6.6 mmol) and PPA (60 g) was treated according to general procedure C, giving 0.630 g (36%) of **7e** as a light-green solid. ^1H NMR (400 MHz, DMSO) δ_{H} (ppm) 12.56 (NH, 1H), 11.81 (NH, 1H), 8.35 (d, $J = 8.7$ Hz, 1H), 8.15 (d, $J = 8.1$ Hz, 1H), 7.73 (d, $J = 1.8$ Hz, 1H), 7.51 (d, $J = 6.2$ Hz, 1H), 7.49 (dd, $J = 7.3, 6.2$ Hz, 1H), 7.30 (dd, $J = 8.7, 1.8$ Hz, 1H), 7.23 (dd, $J = 8.1, 7.3$ Hz, 1H). ^{13}C NMR (100 MHz, DMSO) δ_{C} (ppm) 167.30, 140.02, 139.08, 135.65, 129.40, 128.10, 127.94, 123.64, 121.96, 121.31, 121.15, 119.62, 117.13, 116.14, 113.17. ESI-MS: $[\text{M} + \text{H}]^+ m/z$ 268.94.

3,7-Dichloro-5H-indolo[3,2-b]quinolin-11(10H)-one (7f). Reaction of **6f** (2.0 g, 5.9 mmol) with PPA (60 g) according to general procedure C gave 0.725 g (40%) of **7f** as a brown solid. ^1H NMR (400 MHz, DMSO) δ_{H} (ppm) 12.57 (s, NH), 12.02 (s, NH), 8.33 (d, $J = 8.7$ Hz, 1H), 8.20 (d, $J = 1.7$ Hz, 1H), 7.69 (d, $J = 1.8$ Hz, 1H), 7.54 (d, $J = 8.8$ Hz, 1H), 7.49 (dd, $J = 8.8, 1.7$ Hz, 1H), 7.31 (dd, $J = 8.7, 1.8$ Hz, 1H). ^{13}C NMR (100 MHz, DMSO) δ_{C} (ppm) 167.54, 140.08, 137.34, 136.04, 128.52, 128.03, 127.97, 124.51, 123.73, 121.91, 121.55, 120.41, 117.15, 117.03, 114.91. ESI-MS: $[\text{M} + \text{H}]^+ m/z$ 302.89.

3-Chloro-7-methoxy-5H-indolo[3,2-b]quinolin-11(10H)-one (7g). Reaction of **6g** (1.0 g, 3.0 mmol) with PPA (30 g) according to general procedure C gave 0.242 g (27%) of **7g** as a dark green solid. ^1H NMR (400 MHz, DMSO) δ_{H} (ppm) 12.50 (s, NH), 11.63 (s, NH), 8.33 (d, $J = 8.7$ Hz, 1H), 7.70 (d, $J = 1.7$ Hz, 1H), 7.61 (d, $J = 2.2$ Hz, 1H), 7.44 (d, $J = 9.0$ Hz, 1H), 7.28 (dd, $J = 8.7, 1.7$ Hz, 1H), 7.15 (dd, $J = 9.0, 2.2$ Hz, 1H), 3.87 (s, 3H). ^{13}C NMR (100 MHz, DMSO) δ_{C} (ppm) 167.35, 153.49, 139.99, 135.63, 134.47, 129.17, 127.98, 124.30, 121.75, 121.13, 119.19, 117.00, 115.93, 114.27, 101.51, 55.86.

3-Chloro-7-methyl-5H-indolo[3,2-b]quinolin-11(10H)-one (7h). Reaction of **6h** (1.5 g, 4.7 mmol) with PPA (45 g) according to general procedure C gave 0.697 g (52%) of **7h** as a light green solid. ^1H NMR (400 MHz, DMSO) δ_{H} (ppm) 12.53 (s, NH), 11.67 (s, NH), 8.33 (d, $J = 8.7$ Hz, 1H), 7.92 (s, 1H), 7.72 (d, $J = 1.7$ Hz, 1H), 7.42 (d, $J = 8.5$ Hz, 1H), 7.32 (d, $J = 8.5$ Hz, 1H), 7.28 (dd, $J = 8.7, 1.7$ Hz, 1H), 2.47 (s, 3H). ^{13}C NMR (100 MHz, DMSO) δ_{C} (ppm) 167.23, 139.98, 137.57, 135.55, 129.89, 129.05, 128.31, 127.92, 123.86, 121.88, 121.19, 120.33, 117.07, 116.24, 112.95, 21.61.

General Procedure D: 5,10-Bis[2-(diethylamino)ethyl]-5H-indolo[3,2-b]quinolin-11(10H)-one (2a) and 2-[11-[2-(Diethylamino)ethoxy]-10H-indolo[3,2-b]quinolin-10-yl]-N,N-diethylethanamine (3a). A solution of **7a** (40 mg, 0.17 mmol), K_2CO_3 (352.4 mg, 2.55 mmol, 15 equiv), NaI (101.9 mg, 0.68 mmol, 4 equiv) in dried acetone (15 mL), and 2-chloro-N,N-diethylethanaminium chloride (117.0 mg, 0.68 mmol, 4 equiv) was refluxed overnight. After this period, the solvent was removed at reduced pressure and the remaining solid suspended in H_2O (30 mL). The aqueous solution was extracted with CH_2Cl_2 (3 × 30 mL), and the combined organic extracts, were washed with water, dried with brine and anhydrous Na_2SO_4 , and reduced to small volume. The crude mixture was purified by preparative thin layer chromatography using as eluent CH_2Cl_2 :MeOH (9:1) to afford **2a** (20%) and **3a** (23%). Compounds were crystallized as hydrochlorides with HCl in Et_2O after NMR characterization and obtained as light yellow solids, which were then used in all chemical and biological tests after purity was determined by elemental analysis. (**2a**) ^1H NMR (400 MHz, CDCl_3) δ_{H} (ppm) 8.69 (d, $J = 8.3$ Hz, 1H), 8.25 (d, $J = 8.4$ Hz, 1H), 7.70 (m, 2H), 7.59 (d, $J = 8.3$ Hz, 1H), 7.54 (dd, $J = 8.3, 7.6$ Hz, 1H), 7.34 (dd, $J = 8.3, 7.5$ Hz, 1H), 7.24 (dd, $J = 8.4, 7.6$ Hz, 1H), 5.00

(t, J = 8.0 Hz, 2H), 4.84 (t, J = 7.8 Hz, 2H), 3.03 (t, J = 8.0 Hz, 2H), 2.92 (t, J = 7.8 Hz, 2H), 2.71 (m, 8H), 1.09 (m, 12H). ^{13}C NMR (101 MHz, CDCl_3) δ_{C} (ppm) 169.13, 139.70, 139.65, 131.38, 130.62, 127.32, 126.86, 124.89, 122.69, 122.60, 120.95, 119.52, 115.14, 114.11, 110.63, 53.17, 50.87, 47.69, 47.35, 43.10, 11.85. Anal. (C, H, N): Calcd for $\text{C}_{27}\text{H}_{36}\text{N}_4\text{O}\cdot 2\text{HCl}$: C, 63.24, H, 7.51, N, 10.93, found: C, 63.25, H, 7.34, N, 10.55. (3a) ^1H NMR (400 MHz, CDCl_3) δ_{H} (ppm) 8.55 (d, J = 7.7 Hz, 1H), 8.40 (d, J = 8.2 Hz, 1H), 8.33 (d, J = 8.5 Hz, 1H), 7.70 (dd, J = 8.5, 6.8 Hz, 1H), 7.66 (dd, J = 8.2, 7.4 Hz, 1H), 7.58 (dd, J = 8.2, 6.80 Hz, 1H), 7.52 (d, J = 8.2 Hz, 1H), 7.35 (dd, J = 7.7, 7.4 Hz, 1H), 4.73 (t, J = 7.70 Hz, 2H), 4.32 (t, J = 6.3 Hz, 2H), 3.10 (t, J = 6.3 Hz, 2H), 2.79 (t, J = 7.70 Hz, 2H), 2.70 (q, J = 7.1 Hz, 4H), 2.62 (q, J = 7.1 Hz, 4H), 1.13 (t, J = 7.1 Hz, 6H), 1.00 (t, J = 7.1 Hz, 6H). ^{13}C NMR (101 MHz, CDCl_3) δ_{C} (ppm) 148.59, 145.83, 144.80, 144.58, 129.69, 129.31, 126.65, 124.87, 124.68, 122.46, 122.23, 122.08, 121.27, 119.86, 109.17, 74.51, 52.93, 51.71, 47.69, 47.62, 43.51, 12.06. Anal. (C, H, N): Calcd for $\text{C}_{27}\text{H}_{36}\text{N}_4\text{O}\cdot 2\text{HCl}$: C, 60.65, H, 7.31, N, 10.48, found: C, 61.07, H, 7.61, N, 10.12.

5,10-Bis[2-(pyrrolidin-1-yl)ethyl]-5H-indolo[3,2-b]quinolin-11-(10H)-one (2b) and 11-[2-(Pyrrolidin-1-yl)ethoxy]-10-[2-(pyrrolidin-1-yl)ethyl]-10H-indolo[3,2-b]quinoline (3b). A solution of **7a** (70 mg, 0.29 mmol), K_2CO_3 (619.8 mg, 4.35 mmol, 15 equiv) in dried acetone (20 mL), and 1-(2-chloroethyl)pyrrolidine hydrochloride (203.4 mg, 1.20 mmol, 4 equiv) was refluxed and purified according to procedure D, using as eluent Hex:AcOEt (1:1) to give **2b** (27.3 mg, 21%) and **3b** (45.5 mg, 35%). (2b) ^1H NMR (400 MHz, CDCl_3) δ_{H} (ppm) 8.68 (d, J = 7.8 Hz, 1H), 8.24 (d, J = 8.4 Hz, 1H), 7.72 (m, 2H), 7.69 (d, J = 8.5 Hz, 1H), 7.57 (dd, J = 8.5, 7.2 Hz, 1H), 7.37 (m, 1H), 7.28 (dd, J = 8.4, 7.2 Hz, 1H), 5.13 (t, J = 7.7 Hz, 2H), 4.89 (t, J = 7.8 Hz, 2H), 3.11 (m, 4H), 2.85 (m, 4H), 2.78 (m, 4H), 1.92 (m, 4H), 1.89 (m, 4H). ^{13}C NMR (100 MHz, CDCl_3) δ_{C} (ppm) 169.05, 139.61, 139.51, 131.62, 130.81, 127.70, 126.78, 124.88, 122.50, 122.46, 121.18, 119.95, 115.10, 114.11, 110.65, 55.82, 54.75, 54.24, 53.44, 47.20, 43.21, 23.62, 23.58. Anal. (C, H, N): Calcd for $\text{C}_{27}\text{H}_{32}\text{N}_4\text{O}\cdot 2\text{HCl}\cdot 2\text{H}_2\text{O}$: C, 60.33, H, 7.13, N, 10.42, found: C, 60.76, H, 7.53, N, 10.32. (3b): ^1H NMR (400 MHz, CDCl_3) δ_{H} (ppm) 8.44 (d, J = 7.6 Hz, 1H), 8.22 (d, J = 8.0 Hz, 1H), 8.20 (d, J = 8.0 Hz, 1H), 7.62–7.54 (m, 2H), 7.49 (d, J = 8.0 Hz, 1H), 7.48 (dd, J = 8.0, 8.0 Hz, 1H), 7.25 (ddd, 1H), 4.79 (t, J = 7.5 Hz, 2H), 4.30 (t, J = 5.8 Hz, 2H), 3.03 (t, J = 5.8 Hz, 2H), 2.86 (t, J = 7.5 Hz, 2H), 2.63 (m, 8H), 1.79 (m, 4H), 1.75 (m, 4H). ^{13}C NMR (100 MHz, CDCl_3) δ_{C} (ppm) 148.59, 145.92, 144.58, 144.43, 129.95, 129.37, 126.78, 124.88, 124.62, 122.41, 122.14, 122.09, 121.10, 120.13, 109.24, 74.64, 55.81, 54.76, 54.41, 43.43, 23.60, 23.56. Anal. (C, H, N): Calcd for $\text{C}_{27}\text{H}_{32}\text{N}_4\text{O}\cdot 2\text{HCl}\cdot 3\text{H}_2\text{O}$: C, 58.37, H, 7.26, N, 10.09, found: C, 58.79, H, 7.74, N, 9.72.

5,10-Bis[3-(diethylamino)propyl]-5H-indolo[3,2-b]quinolin-11-(10H)-one (2c) and 3-[11-(3-(Diethylamino)propoxy)-10H-indolo[3,2-b]quinolin-10-yl]-N,N-diethylpropan-1-amine (3c). According to general procedure D, **7a** (100 mg, 0.427 mmol) was reacted with 3-chloro-*N,N*-diethylpropan-1-amine (31.9 mg, 1.71 mmol, 4 equiv). The crude mixture was purified by preparative thin layer chromatography using as eluent Hex:AcOEt (1:1) to give **2c** (53.1 mg, 27%) and **3c** (43.3 mg, 22%, <95% purity). (2c): ^1H NMR (400 MHz, CDCl_3) δ_{H} (ppm) 8.66 (dd, J = 8.3, 1.5 Hz, 1H), 8.25 (d, J = 8.5 Hz, 1H), 7.72 (d, J = 8.6 Hz, 1H), 7.66 (ddd, J = 8.6, 7.5, 1.5 Hz, 1H), 7.57 (d, J = 8.3 Hz, 1H), 7.50 (dd, J = 8.3, 7.6 Hz, 1H), 7.31 (ddd, J = 8.3, 7.5, 0.7 Hz, 1H), 7.20 (ddd, J = 8.5, 7.6, 0.7 Hz, 1H), 4.93 (t, J = 7.3 Hz, 2H), 4.77 (t, J = 8.0 Hz, 2H), 2.68 (t, J = 6.3 Hz, 2H), 2.64–2.56 (m, 6H), 2.53 (q, J = 7.3 Hz, 4H), 2.14 (quint, J = 8.0 Hz, 2H), 2.05 (quint, J = 7.3 Hz, 2H), 1.11 (t, J = 7.1 Hz, 6H), 1.00 (t, J = 7.3 Hz, 6H). ^{13}C NMR (100 MHz, CDCl_3) δ_{C} (ppm) 169.06, 139.64, 139.48, 131.30, 130.69, 127.21, 126.83, 125.00, 122.88, 122.72, 120.89, 119.41, 115.20, 114.29, 110.74, 50.38, 50.14, 47.14, 46.71, 46.60, 43.01, 28.20, 26.51, 11.98, 11.63. ESI-MS: $[\text{M} + \text{H}]^+ m/z$ 461.27. Anal. (C, H, N): Calcd for $\text{C}_{29}\text{H}_{40}\text{N}_4\text{O}\cdot 0.4\text{HCl}$: C, 56.75, H, 7.26, N, 9.13, found: C, 56.76, H, 7.46, N, 8.79. (3c): ^1H NMR (400 MHz, CDCl_3) δ_{H} (ppm) 8.53 (d, J = 7.9 Hz, 1H), 8.31 (d, J = 8.2 Hz, 1H), 8.27 (dd, J = 8.5, 0.8 Hz, 1H), 7.68–7.60 (m, 2H), 7.55 (ddd, J = 8.4, 7.6, 0.7 Hz, 1H), 7.49 (d, J = 8.3 Hz, 1H), 7.32 (dd, J = 7.9, 7.4 Hz, 1H), 4.59 (t, J = 7.5 Hz, 2H), 4.26 (t, J = 6.5 Hz, 2H), 2.80 (t, J = 7.3 Hz, 2H),

2.62 (q, J = 7.1 Hz, 4H), 2.47 (q, J = 7.1 Hz, 6H), 2.23–2.14 (m, 2H), 2.04–1.93 (m, 2H), 1.08 (t, J = 7.1 Hz, 6H), 0.96 (t, J = 7.1 Hz, 6H). ^{13}C NMR (100 MHz, CDCl_3) δ_{C} (ppm) 154.53, 147.13, 141.47, 138.04, 135.73, 133.78, 128.62, 127.20, 124.79, 123.45, 122.50, 121.11, 115.61, 112.71, 77.21, 50.96, 50.35, 48.51, 44.13, 26.63, 26.37, 9.54, 9.38. ESI-MS: $[\text{M} + \text{H}]^+ m/z$ 461.24.

5,10-Bis[3-(piperidin-1-yl)propyl]-5H-indolo[3,2-b]quinolin-11-(10H)-one (2d) and 11-[3-(Piperidin-1-yl)propoxy]-10-[3-(piperidin-1-yl)propyl]-10H-indolo[3,2-b]quinoline (3d). A solution of **7a** (70 mg, 0.29 mmol), K_2CO_3 (619.8 mg, 4.35 mmol, 15 equiv) in dried acetone (20 mL), and 1-(3-chloropropyl)piperidine hydrochloride (237.0 mg, 1.20 mmol, 4 equiv) was reacted and purified according to procedure D, using as eluent Hex:AcOEt (1:1) to give **2d** (45.2 mg, 31%) and **3d** (56.3 mg, 38%). (2d) ^1H NMR (400 MHz, CDCl_3) δ_{H} (ppm) 8.68 (d, J = 8.1 Hz, 1H), 8.24 (d, J = 8.3 Hz, 1H), 7.80 (d, J = 8.6 Hz, 1H), 7.68 (dd, J = 8.6, 7.3 Hz, 1H), 7.65 (d, J = 8.4 Hz, 1H), 7.52 (dd, J = 8.4, 7.4 Hz, 1H), 7.34 (dd, J = 8.1, 7.3 Hz, 1H), 7.22 (dd, J = 8.3, 7.4 Hz, 1H), 4.96 (t, J = 7.1 Hz, 2H), 4.81 (t, J = 7.2 Hz, 2H), 2.53 (t, J = 6.3 Hz, 2H), 2.47 (m, 4H), 2.35 (m, 6H), 2.18 (m, 2H), 2.12 (quint, J = 7.1 Hz, 2H), 1.69 (quint, J = 5.5 Hz, 4H), 1.58 (quint, J = 5.6 Hz, 4H), 1.51 (m, 2H), 1.42 (m, 2H). ^{13}C NMR (100 MHz, CDCl_3) δ_{C} (ppm) 169.03, 139.79, 139.53, 131.21, 130.66, 127.05, 126.73, 124.91, 122.73, 122.70, 120.84, 119.33, 115.08, 114.37, 110.91, 55.97, 55.91, 55.07, 54.54, 54.46, 53.83, 46.25, 42.78, 28.19, 26.20, 25.98, 24.48. Anal. (C, H, N): Calcd for $\text{C}_{31}\text{H}_{40}\text{N}_4\text{O}\cdot 2\text{HCl}\cdot 5\text{H}_2\text{O}$: C, 57.49, H, 8.09, N, 8.65, found: C, 57.45, H, 8.04, N, 8.43. (3d) ^1H NMR (400 MHz, CDCl_3) δ_{H} (ppm) 8.53 (d, J = 7.7 Hz, 1H), 8.32 (d, J = 7.9 Hz, 1H), 8.31 (d, J = 7.8 Hz, 1H), 7.66–7.58 (m, 2H), 7.53 (dd, J = 8.4, 7.8 Hz, 1H), 7.51 (d, J = 7.8 Hz, 1H), 7.30 (dd, J = 7.7, 7.2 Hz, 1H), 4.57 (t, J = 6.9 Hz, 2H), 4.22 (t, J = 6.2 Hz, 2H), 2.65 (t, J = 7.2 Hz, 2H), 2.47 (m, 4H), 2.26 (m, Hz, 6H), 2.20 (quint, J = 6.2 Hz, 2H), 2.02 (quint, J = 6.9 Hz, 2H), 1.64 (quint, J = 5.6 Hz, 4H), 1.54 (quint, J = 5.6 Hz, 4H), 1.49 (m, 2H), 1.40 (m, 2H). ^{13}C NMR (100 MHz, CDCl_3) δ_{C} (ppm) 148.58, 145.76, 144.82, 144.53, 129.54, 129.29, 126.55, 124.74, 124.59, 122.38, 122.18, 121.92, 121.25, 119.68, 109.36, 74.13, 56.12, 55.35, 54.68, 54.53, 42.75, 27.58, 26.91, 26.09, 25.97, 24.52, 24.45. Anal. (C, H, N): Calcd for $\text{C}_{31}\text{H}_{40}\text{N}_4\text{O}\cdot 3\text{HCl}\cdot 3.5\text{H}_2\text{O}$: C, 56.36, H, 8.01, N, 8.55, found: C, 56.66, H, 7.67, N, 8.53.

7-Chloro-5,10-bis[2-(diethylamino)ethyl]-5H-indolo[3,2-b]quinolin-11-(10H)-one (2e) and 2-[[7-Chloro-10-(2-(diethylamino)ethyl)-10H-indolo[3,2-b]quinolin-11-yl]oxy]-N,N-diethylethanamine (3e). According to general procedure D, **7b** (100 mg, 0.372 mmol) was reacted with 2-chloro-*N,N*-diethylethanamine hydrochloride (256.1 mg, 1.488 mmol, 4 equiv). The crude mixture was purified by preparative thin layer chromatography using as eluent Hex:AcOEt (1:1) to give **2e** (40.0 mg, 23%) and **3e** (26.1 mg, 15%). (2e): ^1H NMR (400 MHz, CD_3OD) δ_{H} (ppm) 8.54 (dd, J = 8.2, 1.4 Hz, 1H), 8.43 (d, J = 1.4 Hz, 1H), 8.07 (d, J = 8.8 Hz, 1H), 7.88 (ddd, J = 8.8, 7.8, 1.4 Hz, 1H), 7.82 (d, J = 9.1 Hz, 1H), 7.66 (dd, J = 9.1, 1.4 Hz, 1H), 7.43 (dd, J = 8.2, 7.8 Hz, 1H), 5.37 (t, J = 7.9 Hz, 2H), 5.14 (t, J = 6.4 Hz, 2H), 3.65 (t, J = 6.4 Hz, 2H), 3.56 (t, J = 7.9 Hz, 2H), 3.44–3.36 (m, 8H), 1.42 (t, J = 7.1 Hz, 6H), 1.36 (t, J = 7.3 Hz, 6H). ^{13}C NMR (100 MHz, CD_3OD) δ_{C} (ppm) 170.40, 140.58, 139.90, 134.46, 132.06, 130.45, 127.98, 127.34, 125.53, 124.25, 123.84, 122.91, 117.11, 116.10, 113.40, 53.68, 49.64, 49.40, 49.05, 43.98, 41.50, 9.36. Anal. (C, H, N): Calcd for $\text{C}_{27}\text{H}_{35}\text{ClN}_4\text{O}\cdot 3.7\text{HCl}$: C, 53.87, H, 6.49, N, 9.31, found: C, 53.59, H, 6.58, N, 9.23. (3e): ^1H NMR (400 MHz, CDCl_3) δ_{H} (ppm) 8.48 (d, J = 1.9 Hz, 1H), 8.36 (dd, J = 8.5, 1.1 Hz, 1H), 8.28 (d, J = 8.3 Hz, 1H), 7.66 (ddd, J = 8.3, 7.7, 1.1 Hz, 1H), 7.58–7.53 (m, 2H), 7.41 (d, J = 8.7 Hz, 1H), 4.66 (t, J = 7.3 Hz, 2H), 4.28 (t, J = 6.2 Hz, 2H), 3.05 (t, J = 6.2 Hz, 2H), 2.77 (t, J = 7.3 Hz, 2H), 2.67 (q, J = 7.2 Hz, 4H), 2.56 (q, J = 7.2 Hz, 4H), 1.09 (t, J = 7.2 Hz, 6H), 0.93 (t, J = 7.2 Hz, 6H). ^{13}C NMR (100 MHz, CDCl_3) δ_{C} (ppm) 147.28, 146.03, 144.92, 143.03, 129.58, 129.41, 126.97, 125.44, 125.23, 125.03, 123.61, 122.33, 121.64, 121.30, 110.42, 74.57, 52.97, 51.75, 47.64, 47.55, 43.57, 11.81, 11.77. Anal. (C, H, N): Calcd for $\text{C}_{27}\text{H}_{35}\text{ClN}_4\text{O}\cdot 4.5\text{HCl}$: C, 51.38, H, 6.31, N, 8.88, found: C, 51.32, H, 6.58, N, 8.9.

5,10-Bis[2-(diethylamino)ethyl]-7-methoxy-5H-indolo[3,2-b]quinolin-11-(10H)-one (2f) and 2-[[11-(2-(Diethylamino)ethoxy)-7-methoxy-10H-indolo[3,2-b]quinolin-10-yl]-N,N-diethylethanamine (3f). According to general procedure D, **7c** (100 mg, 0.378 mmol) was

reacted with 2-chloro-*N,N*-diethylethanaminium chloride (260.6 mg, 1.514 mmol, 4 equiv). The crude mixture was purified by preparative thin layer chromatography using as eluent Hex:AcOEt (7:3) to give **2f** (5.25 mg, 3%) and **3f** (14.0 mg, 8%, <95% purity). (**2f**): ^1H NMR (400 MHz, CDCl_3) δ_{H} (ppm) 8.62 (d, J = 8.1 Hz, 1H), 7.91 (d, J = 8.9 Hz, 1H), 7.81–7.65 (m, 3H), 7.40–7.28 (m, 2H), 5.27 (t, J = 6.5 Hz, 2H), 4.84 (t, J = 7.5 Hz, 2H), 3.93 (s, 3H), 3.31 (t, J = 7.5 Hz, 2H), 3.13–2.98 (m, 6H), 2.74 (q, J = 7.0 Hz, 4H), 1.31 (t, J = 6.7 Hz, 6H). ^{13}C NMR (100 MHz, CDCl_3) δ_{C} (ppm) 169.15, 154.27, 139.82, 135.47, 131.75, 130.84, 126.69, 124.63, 123.07, 121.24, 119.05, 115.14, 114.42, 112.10, 104.35, 56.28, 52.15, 51.64, 47.63, 47.58, 46.96, 40.82, 12.29, 11.67. Anal. (C, H, N): Calcd for $\text{C}_{28}\text{H}_{38}\text{N}_4\text{O}_2 \cdot 4.6\text{HCl}$: C, 53.35, H, 6.83, N, 8.89, found: C, 53.45, H, 6.59, N, 8.86. (**3f**): ^1H NMR (400 MHz, CDCl_3) δ_{H} (ppm) 8.33 (d, J = 8.6 Hz, 1H), 8.30 (d, J = 8.6 Hz, 1H), 7.97 (s, 1H), 7.66 (dd, J = 8.6, 7.3 Hz, 1H), 7.56 (dd, J = 8.6, 7.3 Hz, 1H), 7.50 (d, J = 8.8 Hz, 1H), 7.29 (d, J = 8.8 Hz, 1H), 4.83 (bt, 2H), 4.33 (t, J = 5.7 Hz, 2H), 3.97 (s, 3H), 3.10 (t, J = 5.7 Hz, 2H), 2.88 (bt, 2H), 2.78–2.68 (m, 8H), 1.12 (t, J = 7.0 Hz, 6H), 1.05 (t, J = 6.6 Hz, 6H). ^{13}C NMR (100 MHz, CDCl_3) δ_{C} (ppm) 154.82, 148.58, 145.99, 139.32, 129.50, 127.73, 127.16, 126.00, 125.29, 123.09, 121.93, 121.11, 120.30, 110.61, 103.90, 73.29, 56.24, 52.77, 50.76, 47.50, 47.36, 40.90, 11.25, 11.10. ESI-MS: $[\text{M} + \text{H}]^+ m/z$ 463.20.

5,10-Bis[2-(diethylamino)ethyl]-7-methyl-5H-indolo[3,2-*b*]quinolin-11(10*H*)-one (2g) and 2-[11-[2-(Diethylamino)ethoxy]-7-methyl-10*H*-indolo[3,2-*b*]quinolin-10-yl]-*N,N*-diethylethanamine (3g). According to general procedure D, **7d** (100 mg, 0.403 mmol) was reacted with 2-chloro-*N,N*-diethylethanaminium chloride (277.4 mg, 1.612 mmol, 4 equiv). The crude mixture was purified by preparative thin layer chromatography using as eluent Hex:AcOEt (1:1) to give **2g** (16.2 mg, 9%), and **3g** (30.6 mg, 17%, <95% purity). (**2g**): ^1H NMR (400 MHz, CDCl_3) δ_{H} (ppm) 8.68 (dd, J = 8.5, 0.8 Hz, 1H), 8.03 (s, 1H), 7.72–7.64 (m, 2H), 7.48 (d, J = 8.6 Hz, 1H), 7.37 (dd, J = 8.6, 0.8 Hz, 1H), 7.37 (ddd, J = 8.5, 7.1, 1.5 Hz, 1H), 4.97 (t, J = 7.6 Hz, 2H), 4.81 (t, J = 7.8 Hz, 2H), 3.03 (t, J = 7.8 Hz, 2H), 2.90 (t, J = 7.6 Hz, 2H), 2.74 (q, J = 7.1 Hz, 4H), 2.69 (q, J = 7.2 Hz, 2H), 2.53 (s, 3H), 1.13 (t, J = 7.1 Hz, 6H), 1.07 (t, J = 7.2 Hz, 6H). ^{13}C NMR (100 MHz, CDCl_3) δ_{C} (ppm) 169.14, 139.68, 138.36, 131.43, 130.39, 129.32, 128.91, 126.94, 124.87, 122.96, 122.04, 120.96, 115.28, 114.11, 110.40, 53.21, 50.78, 47.82, 47.65, 47.33, 43.07, 21.69, 12.14, 12.05. Anal. (C, H, N): Calcd for $\text{C}_{28}\text{H}_{38}\text{N}_4 \cdot 2\text{HCl} \cdot 2\text{H}_2\text{O}$: C, 62.56, H, 7.89, N, 10.42, found: C, 62.83, H, 8.10, N, 10.75. (**3g**): ^1H NMR (400 MHz, CDCl_3) δ_{H} (ppm): 8.36 (dd, J = 8.4, 1.2 Hz, 1H), 8.33 (s, 1H), 8.29 (d, J = 8.4 Hz, 1H), 7.64 (ddd, J = 8.4, 7.6, 1.2 Hz, 1H), 7.54 (ddd, J = 8.4, 7.6, 1.3 Hz, 1H), 7.46 (dd, J = 8.3, 1.3 Hz, 1H), 7.38 (d, J = 8.3 Hz, 1H), 4.66 (t, J = 7.6 Hz, 2H), 4.28 (t, J = 6.3 Hz, 2H), 3.06 (t, J = 6.3 Hz, 2H), 2.75 (t, J = 7.6 Hz, 2H), 2.67 (q, J = 7.1 Hz, 4H), 2.59 (q, J = 7.1 Hz, 4H), 2.55 (s, 3H), 1.10 (t, J = 7.1 Hz, 6H), 0.98 (t, J = 7.1 Hz, 6H). ^{13}C NMR (100 MHz, CD_3OD) δ_{C} (ppm): 137.35, 133.39, 131.55, 131.24, 128.89, 128.78, 124.41, 123.94, 123.79, 122.52, 120.47, 117.59, 110.13, 73.20, 52.68, 49.12, 48.57, 40.13, 19.73, 9.18, 9.27. ESI-MS: $[\text{M} + \text{H}]^+ m/z$ 447.34.

3-Chloro-5,10-bis[2-(diethylamino)ethyl]-5*H*-indolo[3,2-*b*]quinolin-11(10*H*)-one (2h) and 2-[3-Chloro-10-(2-(diethylamino)ethyl)-10*H*-indolo[3,2-*b*]quinolin-11-yl]oxy-*N,N*-diethylethanamine (3h). According to general procedure D, **7e** (40 mg, 0.118 mmol) was reacted with 2-chloro-*N,N*-diethylethanaminium chloride (64.5 mg, 0.472 mmol, 4 equiv). The crude mixture was purified by preparative thin layer chromatography using as eluent Hex:AcOEt (1:1) to give **2h** (11.6 mg, 21%) and **3h** (18.3 mg, 33%). (**2h**): ^1H NMR (400 MHz, CDCl_3) δ_{H} (ppm) 8.57 (d, J = 8.7 Hz, 1H), 8.18 (d, J = 8.4 Hz, 1H), 7.72 (d, J = 1.6 Hz, 1H), 7.59 (d, J = 8.4 Hz, 1H), 7.54 (dd, J = 8.4 Hz, 1H), 7.27 (dd, J = 8.7, 1.6 Hz, 1H), 7.23 (d, J = 8.8 Hz, 1H), 4.97 (t, J = 7.3 Hz, 2H), 4.77 (t, J = 7.4 Hz, 2H), 3.02 (d, J = 7.4 Hz, 2H), 2.90 (t, J = 7.3 Hz, 2H), 2.69 (q, J = 7.1 Hz, 8H), 1.07 (t, J = 7.1 Hz, 6H), 1.06 (t, J = 7.2 Hz, 6H). ^{13}C NMR (100 MHz, CDCl_3) δ_{C} (ppm) 168.61, 140.36, 139.72, 137.70, 130.62, 128.43, 127.56, 123.26, 122.78, 122.46, 121.66, 119.84, 115.05, 114.33, 110.77, 53.12, 51.10, 47.73, 47.67, 47.57, 43.08, 12.03. Anal. (C, H, N): Calcd for $\text{C}_{27}\text{H}_{35}\text{ClN}_4\text{O} \cdot 3.4\text{HCl}$: C, 54.87, H, 6.55, N, 9.48, found: C, 54.90,

H, 6.68, N, 9.38. (**3h**): ^1H NMR (400 MHz, CDCl_3) δ_{H} (ppm) 8.51 (d, J = 7.7 Hz, 1H), 8.39 (d, J = 9.0 Hz, 1H), 8.32 (d, J = 1.9 Hz, 1H), 7.67 (dd, J = 7.3 Hz, 1H), 7.51 (m, 2H), 7.35 (dd, J = 7.7, 7.3 Hz, 1H), 4.69 (t, J = 7.5 Hz, 2H), 4.28 (t, J = 6.1 Hz, 2H), 3.06 (t, J = 6.1 Hz, 2H), 2.80 (t, J = 7.5 Hz, 2H), 2.69 (q, J = 7.1 Hz, 4H), 2.60 (q, J = 7.1 Hz, 4H), 1.12 (t, J = 7.1 Hz, 6H), 0.98 (t, J = 7.1 Hz, 6H). ^{13}C NMR (100 MHz, CDCl_3) δ_{C} (ppm) 149.45, 146.03, 144.92, 144.70, 132.34, 130.02, 128.00, 125.54, 124.95, 122.86, 122.23, 122.18, 120.68, 120.05, 109.29, 74.92, 53.04, 51.76, 47.71, 47.63, 43.60, 12.10, 11.91. Anal. (C, H, N): Calcd for $\text{C}_{27}\text{H}_{35}\text{ClN}_4\text{O} \cdot 4.2\text{HCl}$: C, 52.29, H, 6.37, N, 9.03, found: C, 52.37, H, 6.56, N, 8.95.

3,7-Dichloro-5,10-bis[2-(diethylamino)ethyl]-5*H*-indolo[3,2-*b*]quinolin-11(10*H*)-one (2i) and 2-[3,7-Dichloro-10-(2-(diethylamino)ethyl)-10*H*-indolo[3,2-*b*]quinolin-11-yl]oxy-*N,N*-diethylethanamine (3i). According to general procedure D, **7f** (40 mg, 0.13 mmol) was reacted with 2-chloro-*N,N*-diethylethanaminium chloride (72.1 mg, 5.28 mmol, 4 equiv). The crude mixture was purified by preparative thin layer chromatography, using as eluent Hex:AcOEt (6:4) to give **2i** (12.6 mg, 19%) and **3i** (22.5 mg, 34%). (**2i**): ^1H NMR (400 MHz, CDCl_3) δ_{H} (ppm) 8.57 (d, J = 8.7 Hz, 1H), 8.27 (d, J = 1.6 Hz, 1H), 7.72 (d, J = 1.6 Hz, 1H), 7.57 (t, J = 10.5 Hz, 1H), 7.51 (dd, J = 9.0, 1.7 Hz, 1H), 7.30 (d, J = 8.7 Hz, 1H), 4.96 (t, J = 7.4 Hz, 2H), 4.72 (t, J = 7.8 Hz, 2H), 3.04 (t, J = 7.8 Hz, 2H), 2.92 (t, J = 7.4 Hz, 2H), 2.71 (q, J = 7.1 Hz, 8H), 1.13 (t, J = 7.1 Hz, 6H), 1.05 (t, J = 7.1 Hz, 6H). ^{13}C NMR (100 MHz, CDCl_3) δ_{C} (ppm) 168.73, 140.44, 138.04, 137.96, 129.74, 128.43, 127.82, 125.38, 123.32, 123.18, 121.84, 121.76, 115.68, 114.30, 111.96, 53.22, 50.91, 47.78, 47.53, 43.35, 11.93. Anal. (C, H, N): Calcd for $\text{C}_{27}\text{H}_{34}\text{Cl}_2\text{N}_4\text{O} \cdot 2.8\text{HCl}$: C, 53.72, H, 6.16, N, 9.28, found: C, 53.65, H, 5.95, N, 9.21. (**3i**): ^1H NMR (400 MHz, CDCl_3) δ_{H} (ppm) 8.45 (d, J = 2.0 Hz, 1H), 8.37 (d, J = 9.0 Hz, 1H), 8.26 (d, J = 2.0 Hz, 1H), 7.59 (dd, J = 8.7, 2.0 Hz, 1H), 7.50 (dd, J = 9.0, 2.0 Hz, 1H), 7.42 (d, J = 8.7 Hz, 1H), 4.69 (t, J = 7.3 Hz, 2H), 4.27 (t, J = 6.0 Hz, 2H), 3.05 (t, J = 6.0 Hz, 2H), 2.77 (t, J = 7.3 Hz, 2H), 2.69 (q, J = 7.1 Hz, 4H), 2.56 (q, J = 7.1 Hz, 4H), 1.12 (t, J = 7.1 Hz, 6H), 0.93 (t, J = 7.1 Hz, 6H). ^{13}C NMR (100 MHz, CDCl_3) δ_{C} (ppm) 148.10, 146.15, 145.09, 143.16, 132.65, 129.86, 128.04, 125.87, 125.56, 125.36, 123.33, 122.91, 121.72, 120.80, 110.48, 75.06, 53.07, 51.88, 47.69, 47.58, 43.88, 12.07, 11.89. Anal. (C, H, N): Calcd for $\text{C}_{27}\text{H}_{34}\text{Cl}_2\text{N}_4\text{O} \cdot 3.2\text{HCl}$: C, 52.46, H, 6.08, N, 9.07, found: C, 52.57, H, 5.67, N, 8.74.

3-Chloro-10-[2-(diethylamino)ethyl]-5-[3-(diethylamino)propyl]-7-methoxy-5*H*-indolo[3,2-*b*]quinolin-11(10*H*)-one (2j) and 2-[3-Chloro-10-(2-(diethylamino)ethyl)-7-methoxy-10*H*-indolo[3,2-*b*]quinolin-11-yl]oxy-*N,N*-diethylethanamine (3j). A solution of **7g** (70 mg, 0.23 mmol), K_2CO_3 (476 mg, 3.45 mmol, 15 equiv) in dried acetone (20 mL), and 2-chloro-*N,N*-diethylethanaminium chloride (159.3 mg, 0.92 mmol, 4 equiv) was reacted and purified according to procedure D, using as eluent Hex:AcOEt (3:2) to give **2j** (20.3 mg, 17%) and **3j** (39.4 mg, 34%). (**2j**): ^1H NMR (400 MHz, CDCl_3) δ 8.56 (d, J = 8.7 Hz, 1H), 7.70 (dd, J = 4.3, 2.0 Hz, 2H), 7.60 (d, J = 9.0 Hz, 1H), 7.27 (dd, J = 3.3, 2.1 Hz, 1H), 7.26–7.24 (m, 1H), 5.00 (t, J = 7.3 Hz, 2H), 4.75 (t, J = 7.3 Hz, 2H), 3.93 (s, 3H), 3.13–3.03 (q, J = 7.3 Hz, 2H), 2.98 (d, J = 7.3 Hz, 2H), 2.73 (dq, J = 7.2 Hz, 8H), 1.09 (dt, J = 7.2 Hz, 12H). ^{13}C NMR (101 MHz, CDCl_3) δ 168.64, 153.99, 140.38, 137.74, 135.42, 128.40, 123.29, 123.01, 121.53, 120.23, 118.67, 114.78, 114.23, 111.75, 103.87, 56.13, 53.03, 51.65, 47.78, 47.47, 42.67, 11.73. Anal. (C, H, N): Calcd for $\text{C}_{28}\text{H}_{37}\text{ClN}_4\text{O}_2 \cdot 2.2\text{HCl} \cdot 0.7\text{H}_2\text{O}$: C, 57.01; H, 6.94; N, 9.50, found: C, 57.38; H, 6.71; N, 9.35. (**3j**): ^1H NMR (400 MHz, CDCl_3) δ 8.35 (d, J = 9.0 Hz, 1H), 8.28 (d, J = 2.0 Hz, 1H), 7.94 (d, J = 2.5 Hz, 1H), 7.47 (dd, J = 9.0, 2.1 Hz, 1H), 7.41 (d, J = 8.9 Hz, 1H), 7.28 (dd, J = 8.9, 2.6 Hz, 1H), 4.65 (t, J = 7.2 Hz, 2H), 4.25 (t, J = 6.3 Hz, 2H), 3.97 (s, 3H), 3.02 (t, J = 6.3 Hz, 2H), 2.75 (t, J = 7.2 Hz, 2H), 2.66 (q, J = 7.1 Hz, 4H), 2.57 (q, J = 7.1 Hz, 4H), 1.09 (t, J = 7.1 Hz, 6H), 0.95 (t, J = 7.1 Hz, 6H). ^{13}C NMR (101 MHz, CDCl_3) δ 154.31, 149.23, 145.79, 144.83, 139.91, 132.28, 127.91, 125.51, 125.47, 122.88, 122.49, 120.59, 120.18, 110.45, 103.44, 74.78, 56.09, 53.05, 51.76, 47.69, 47.60, 43.61, 11.98, 11.88. Anal. (C, H, N): Calcd for $\text{C}_{28}\text{H}_{37}\text{ClN}_4\text{O}_2 \cdot 2.1\text{HCl} \cdot 1.2\text{H}_2\text{O}$: C, 56.31; H, 7.34; N, 9.38, found: C, 57.37; H, 7.66; N, 9.27.

3-Chloro-5,10-bis[2-(diethylamino)ethyl]-7-methyl-5H-indolo[3,2-b]quinolin-11(10H)-one (2k) and 2-[3-Chloro-10-(2-(diethylamino)ethyl)-7-methyl-10H-indolo[3,2-b]quinolin-11-yl]-oxy-N,N-diethylethanamine (3k). A solution of 7h (80 mg, 0.28 mmol), K_2CO_3 (580 mg, 4.20 mmol, 15 equiv) in dried acetone (20 mL), and 2-chloro-N,N-diethylethanaminium chloride (192.7 mg, 1.12 mmol, 4 equiv) was reacted and purified according to procedure D, using as eluent Hex:AcOEt (3:2) to give **2k** (26.3 mg, 19%) and **3k** (47.2 mg, 35%). (**2k**): mp 220–222 °C; 1H NMR (400 MHz, $CDCl_3$) δ_H (ppm) 8.36 (d, J = 8.7 Hz, 1H), 7.77 (s, 1H), 7.48 (d, J = 1.6 Hz, 1H), 7.28 (d, J = 8.6 Hz, 1H), 7.17 (d, J = 8.6 Hz, 1H), 7.05 (dd, J = 8.7, 1.67 Hz, 1H), 4.74 (t, J = 7.2 Hz, 2H), 4.54 (t, J = 7.2 Hz, 2H), 2.81 (t, J = 7.2 Hz, 2H), 2.68 (t, J = 7.2 Hz, 2H), 2.51 (q, J = 7.1 Hz, 4H), 2.48 (q, J = 7.1 Hz, 4H), 2.32 (s, 3H), 0.90 (t, J = 7.1 Hz, 6H), 0.85 (t, J = 7.1 Hz, 6H). ^{13}C NMR (100 MHz, $CDCl_3$) δ_C (ppm) 168.55, 140.29, 138.29, 137.60, 130.23, 129.42, 129.11, 128.44, 123.17, 122.96, 121.77, 121.51, 115.10, 114.16, 110.45, 53.13, 50.86, 47.77, 47.57, 43.06, 21.62, 12.05, 11.97. Anal. (C, H, N): Calcd for $C_{28}H_{37}N_4O \cdot 2HCl \cdot 3.5H_2O$: C, 54.50, H, 7.51, N, 9.08 found: C, 54.60, H, 7.57, N, 9.31. (**3k**): mp 254–256 °C; 1H NMR (400 MHz, $CDCl_3$) δ_H (ppm) 8.27 (d, J = 9.0 Hz, 1H), 8.20 (s, 1H), 8.19 (d, J = 2.1 Hz, 1H), 7.40–7.36 (m, 2H), 7.29 (d, J = 8.4 Hz, 1H), 4.54 (t, J = 7.6 Hz, 2H), 4.16 (t, J = 6.1 Hz, 2H), 2.94 (t, J = 6.1 Hz, 2H), 2.66 (t, J = 7.6 Hz, 2H), 2.58 (q, J = 7.1 Hz, 4H), 2.50 (q, J = 7.1 Hz, 4H), 2.47 (s, 3H), 1.01 (t, J = 7.1 Hz, 6H), 0.88 (t, J = 7.1 Hz, 6H). ^{13}C NMR (100 MHz, $CDCl_3$) δ_C (ppm) 149.39, 145.91, 144.55, 143.27, 132.18, 131.37, 129.57, 127.97, 125.41, 125.21, 122.84, 122.32, 121.98, 120.65, 109.02, 74.82, 53.04, 51.71, 47.71, 47.63, 43.60, 21.16, 12.11, 11.91. Anal. (C, H, N): Calcd for $C_{28}H_{37}N_4O \cdot 2HCl$: C, 60.70, H, 7.10, N, 10.11, found: C, 60.48, H, 6.97, N, 9.87.

In Vitro Intraerythrocytic Cytostatic Antiplasmodial Activity.

Human red blood cells infected with 1% ring stage *P. falciparum* strains synchronized with 5% sorbitol were incubated with test compounds in 96-well plates at 37 °C for 48 h in RPMI-1640 medium, supplemented with 25 mM HEPES pH 7.4, 0.5% Albumax, 2% human serum, and 100 μ M hypoxanthine, under an atmosphere of 3% O_2 , 5% CO_2 , 91% N_2 . After 48 h, the cells were fixed in 2% formaldehyde in PBS, transferred into PBS with 100 mM NH_4Cl , 0.1% Triton X-100, and 1 nM YOYO-1, and then analyzed in a flow cytometer (FACSort, Beckton Dickinson; EX 488 nm, EM 520 nm). Values of IC_{50} were calculated using GraphPad PRISM software.

In Vitro Intraerythrocytic Cytocidal Activity. Chloroquine-sensitive 3D7 and chloroquine-resistant Dd2 clones were cultured in human erythrocytes and synchronized (when needed) with D-sorbitol before experiments as described previously.⁵⁰ Antiplasmodial cytotoxic (cell killing, quantified by the half-maximal lethal dose or LD_{50}) activity was assessed as previously described,³ with minor modifications. The cytotoxic assay utilizes a 2 or 6 h incubation with high concentrations of drug followed by washing and growth in the absence of drug for 48 h.^{3,14} Stock solutions of test compounds were prepared in water or DMSO. All stocks were then diluted with complete culture medium to achieve the required concentrations. Test compounds were then placed in triplicate wells of 96-well flat-bottom tissue culture plates and serially diluted in asynchronous or sorbitol-synchronized *P. falciparum* culture (1% parasitaemia, 3% final hematocrit) in a final well volume of 100 μ L. To assess the stage specificity of compounds, LD_{50} s were determined after incubations of 2 h and 6 h (under standard culture conditions) at different stages of parasite development: ring (10–16 h post invasion), trophozoite (22–30 h post invasion), and schizont (34–40 h post invasion). Plates were centrifuged at 700G for 5 min. Supernatant was discarded, cell pellets were washed three times with 200 μ L of drug-free medium, and pellet cells were resuspended in 100 μ L of drug-free medium and returned to standard culture conditions for 48 h. After parasites were stained with SYBR Green I (Sigma-Aldrich) (0.002% v/v in PBS) for 30 min under standard culture conditions, fluorescence (excitation and emission of 485 and 538 nm, respectively) was measured with a microplate reader (TRIAD Multimode Detector, DYNEX Technologies). To estimate the LD_{50} , fluorescence readings for each concentration were normalized relative to the positive control wells (no drug added)

and plotted against the logarithm of the different drug dilutions. Correspondent LD_{50} values were estimated from dose–response curves generated using GraphPad Prism 5.

In Vitro Cytotoxicity to Human Cells. HepG2 A16 human hepatic cell line viability was determined based on the MTT assay. An in vitro culture of HepG2 cells was maintained in standard culture conditions. Briefly, cells were seeded in a flat-bottomed 96-well tissue culture plate at a density of 1×10^4 cells/well and allowed to adhere overnight. After removing the medium, 200 μ L of fresh medium containing seven 10-fold dilutions (100 μ M to 1 nM) of each compound were added, and a negative control was performed by adding 200 μ L of drug free medium. The plate was incubated for 24 h under standard culture conditions, medium was then substituted by fresh medium containing identical concentrations of the compounds, and the plates were incubated another 24 h. At the end of the incubation period (48 h), 20 μ L of 3-(4,5-dimethylthiazol-2-yl)-2,5-diphenyl-2H-tetrazolium (MTT; 5 mg/mL in PBS) was added to each well, wells were incubated for 3 h at standard culture conditions, supernatant was removed, and 200 μ L of acidified 2-propanol was added to each well. Absorbance was read at 570 nm, to produce a log dose-dependence curve. The IC_{50} was estimated for each compound by nonlinear interpolation of the dose-dependence curve.

DNA Binding. The binding affinity of compounds 2 and 3 to DNA was assessed by a fluorescence resonance energy transfer (FRET) melting assay. The labeled hairpin DNA sequence 5'-FAM-TATATCTATATTTTTTTATAGCTATA-TAMRA-3' (Eurogentec Ltd., UK) was used. Oligonucleotide was initially diluted to 100 μ M in nuclease free water (not DEPC-treated), purchased from Ambion Applied Biosystems UK. Stock solutions of 20 μ M and subsequent dilutions were obtained in FRET buffer (60 mM KCl, K-cacodylate, pH 7.4). The DNA sequence was diluted from stock to the correct concentration (0.4 μ M). Test compounds were prepared as 10 mM DMSO stock solutions and diluted to 1 mM using 1 mM HCl in HPLC-grade water. Further dilutions were performed using FRET buffer. DNA (50 μ L) and test compound solution (50 μ L) were distributed across 96-well RT-PCR plates (BioRad; MJ Research, Waltham, MA). Fluorescence readings were made with excitation at 450–495 nm and detection at 515–545 nm, taken at intervals of 0.5 °C in the range 30–100 °C, with a constant temperature being maintained for 30 s prior to each reading to ensure a stable value. Final analysis of the data was carried out with GraphPad Prism 5.0 software (GraphPad Software, Inc.). The advanced curve-fitting function in GraphPad Prism was used for calculation of ΔT_m values.

Microscopic Examination of Intraerythrocytic Parasite Development. *P. falciparum* clone 3D7 was cultured in human erythrocytes and synchronized twice with D-sorbitol before experiments as described previously.⁵⁰ Synchronized parasite cultures at ring stage (with 5% hematocrit and 1% parasitaemia) were treated for 24 h with serial dilutions of 2i, 3i, CQ, and MQ. After this incubation period, thin blood smears were prepared from control and treated wells, fixed with methanol, and Giemsa stained (20% Giemsa in water for 15 min). The slides were observed, parasitaemia was determined, and slides were photographed using an optical microscope (Olympus, U-DO). To estimate the IC_{50} , the parasitaemia determined for each concentration was normalized relative to the positive control wells (no drug added) and plotted against the logarithm of the different drug dilutions. Corresponding IC_{50} values were estimated from dose–response curves generated using GraphPad Prism 5.

Intraerythrocytic Growth Inhibition Stage Specificity. Highly synchronized *P. falciparum* (3D7) cultures at ring (10–16 h post invasion), trophozoite (22–30 h post invasion), and schizont (34–40 h post invasion) stages were treated with the selected compound 3i at their respective IC_{99} (33.5 nM) determined by light microscopy as described above. Drug pressures were maintained over 48, 24, and 8 h for ring, trophozoite, and schizont stages, respectively. After the respective incubation periods, thin blood smears were prepared from control and treated wells and processed for Giemsa staining as described above. The percentage of stage-specific inhibition by each compound was calculated in comparison to the corresponding drug

free control by counting at least 3000 cells for each stage. Parasites with pyknotic morphology were considered nonviable cells.

Heme Binding Studies. Titrations of compounds with FPIX-OH in buffered 40% DMSO (v/v) at pH 5.5 were made according to the following procedure. Stock solutions of hematin and ligands were obtained by dissolving compounds in UV-spectroscopy grade DMSO to a concentration of 1 mM, with storage in the dark. Aqueous buffered DMSO (40% v/v, 1 mL) solutions of hematin, CQ, and compounds 2 and 3 were prepared daily from stock solution (100 μ M). Hematin solutions (10 μ M) were prepared with buffered 40% DMSO (v/v) solution and transferred to cuvettes. Solutions of CQ and compounds 2 and 3 (100 μ M) were initially added to the cuvettes in amounts as small as 2 μ L, gradually increasing the volume in subsequent additions until final concentrations higher than the hematin concentration were achieved. After each addition, the cuvette was stirred for 1 min before the absorbance was read. UV-visible titrations were performed between 230 and 500 nm to incorporate the Soret band of porphyrin. The UV-visible spectrum obtained after each titrated addition was analyzed and stacked against the corresponding absorbances. Dissociation constants of compounds complexed with FPIX-OH were determined by fitting the experimental data to the appropriate equation models⁵¹ using least-squares nonlinear regression analysis with GraphPad PRISM software. Models were analyzed by χ -squared parameters. Association constants, K_{ass} , were calculated from dissociation constants.

β -Hematin Inhibition Assay. β -Hematin inhibitory activity was assessed based on differential solubility of β -hematin compared to hematin in DMSO according to the method described by Basilico et al.³⁴ with modifications. Hemin (ferriprotoporphyrin IX chloride), chloroquine diphosphate, and mefloquine hydrochloride were purchased from Sigma–Aldrich. Dimethyl sulfoxide (DMSO) and glacial acetic acid (AcOH) were purchased from Merck. Briefly, 100 μ L of a 4 mM solution of hemin chloride dissolved in 0.1 M NaOH was distributed in 96-well U-bottom microplates to which 50 μ L of drug solution was added. All compounds were dissolved in DMSO, whereas CQ was prepared in distilled water. Serial dilutions were then made with water. The final concentration of DMSO per well did not exceed 6%. In control wells either water or DMSO was added. To initiate β -hematin formation, 50 μ L of acetic acid was added and the plates were incubated at 37 °C for 24 h to allow for complete reaction. After centrifugation (4000 rpm, 15 min), the soluble fraction of unprecipitated material was discarded and the remaining pellet washed once with 200 μ L of DMSO. The plates were centrifuged again, and the residual pellet, consisting of a pure precipitate of β -hematin, was dissolved in 200 μ L of 0.1 M NaOH. An aliquot was transferred onto a 96-well plate, and serial 4-fold dilutions in 0.1 M NaOH were made. The amount of hematin in each well was determined by measuring the absorbance at 405 nm using a TRIAD series multimode detector (Dynex Technologies). The drug concentration required to inhibit β -hematin formation 50% (IC_{50}) was determined using GraphPad Prism software. The data are expressed as means \pm SD from at least two independent experiments.

Determination of Distribution Coefficients (log D), VAR, and LAR. Distribution coefficients were determined by the n -octanol–phosphate buffer (pH = 7.4 or 5.2) partitioning method. n -Octanol was presaturated with adequate phosphate buffer (1%), and vice versa for 48 h. Methanolic stock solutions of 1 mg/mL were prepared for each compound, and an aliquot of these stock solutions was dissolved in appropriate buffer to obtain a final concentration of 100 μ g/mL or 40 μ g/mL in the case of CQ. In three screw-capped tubes, 1000 μ L of the phosphate buffer solution (V_{aq}) was then added to 200 μ L of n -octanol (V_{oct}). In the case of CQ the V_{oct} = 1000 μ L, and in the case of compound 1b the V_{oct} = 100 μ L. The mixtures were shaken by vortex for 2 min, followed by centrifugation at 13000 rpm for 10 min. Determination of compound concentrations in the aqueous phase was performed by HPLC-UV at 275 or 293 nm for 2i and 320 nm for CQ. The column used was a LiCrospher 100 RP-18 (4 \times 125 mm; 5 μ m particle size), with mobile phases consisting of CH_3CN –phosphate buffer pH 3 (13:87) for CQ or CH_3CN –MeOH–phosphate buffer (pH 5.2–6) mixtures for compounds 2 and 3 (Table S5, Supporting

Information). Twenty microliters of the aqueous phase was injected into the chromatographic column, leading to the determination of a peak area before partitioning (W_0) and after partitioning (W_1). This procedure was performed for all samples for three consecutive days. The final W_1 corresponds to the average of three independent measures per day for each partitioning experiment. The log D values consist of the average of the three log D values obtained. Each log D was calculated using the following equation:

$$\log D = \log[(W_0 - W_1)V_{\text{aq}}/W_1V_{\text{oct}}] \quad (1)$$

Vacuolar accumulation ratios (VAR), determined as the compound accumulation ratio from the erythrocytic plasma or parasite cytosol (pH = 7.4) to vacuolar water (pH = 5.2), were calculated from eq 2, whereas the lipid accumulation ratios (LAR), that is the distribution of the drug neutral form between the aqueous phase and the lipid phase, were calculated from eq 3.⁴¹

$$\text{VAR} = \text{antilog}(\log D_{7.4} - \log D_{5.2}) \quad (2)$$

$$\text{LAR} = \text{antilog}(\log D_{7.4}) \quad (3)$$

■ ASSOCIATED CONTENT

■ Supporting Information

¹H and ¹³C NMR data of compounds 2a and 3a and complete chemical shifts assignments (Figure S1); plots of correlations between $\text{pIC}_{50}/\text{pLD}_{50}$ against *P. falciparum* and ClogP (Figure S2), between cytotoxicity of 2 and 3 to human cell line and ClogP (Figure S3), between experimental log $D_{7.4}$ and ClogP (Figure S8); parasitemia dose–response curves (Figure S4); data from equilibrium binding studies with hematin (determination of stoichiometry (Figure S6) and association constants of complexes (Figure S5)); dose–response plot of β -hematin crystallization inhibition by chloroquine (Figure S7); and energy minimized structures of 2a,d and 3a,d showing distances (Å) between side-chain-protonated amine groups (Figure S9). Physicochemical properties of compounds 2a–k and 3a–k, LD_{50} values of compounds against rings, trophozoites, and schizonts, and HPLC elution systems used for determination of compound log D values (Tables S2–S5). This material is available free of charge via the Internet at <http://pubs.acs.org>.

■ AUTHOR INFORMATION

Corresponding Author

*Phone: +351 217946473. E-mail: mapaulo@ff.ul.pt.

Author Contributions

The manuscript was written through contributions of all authors. All authors have given approval to the final version of the manuscript.

Notes

The authors declare no competing financial interest.

■ ACKNOWLEDGMENTS

This work was supported by Fundação para a Ciência e Tecnologia (FCT) through project grants: PTDC/SAU-FAR/114864/2009 and PEst-OE/SAU/UI4013/2014. J. Lavrado thanks FCT for a postdoctoral grant (SFRH/BPD/72903/2010) and S. A. Santos for a Ph.D. grant (SFRH/BD/80162/2011). Authors acknowledge Professor Virgílio do Rosário (IHMT, UNL, Portugal) for the important scientific contribution to this research project and Professor Leslie Leiserowitz (Weizmann Institute of Science, Rehovot, Israel) for helpful comments on drug–hemozoin crystal interactions.

■ ABBREVIATIONS USED

ClogP, calculated logarithm of partition coefficient; CQ, chloroquine; DV, digestive vacuole; Hz, hemozoin; LAR, lipid accumulation ratio; log *D*, logarithm of distribution coefficient; MQ, mefloquine; PfCRT, *Plasmodium falciparum* chloroquine resistance transporter; RI, resistance index; VAR, vacuole accumulation ratio

■ REFERENCES

- (1) Alonso, P. L.; Djimde, A.; Kremsner, P.; Magill, A.; Milman, J.; Najera, J.; Plowe, C. V.; Rabinovich, R.; Wells, T.; Yeung, S. The malERA Consultative Group on Drugs. A research agenda for malaria eradication: drugs. *PLoS Med.* **2011**, *8*, e1000402.
- (2) Burrows, J. N.; van Huijsduijnen, R. H.; Mohrle, J. J.; Oeuvray, C.; Wells, T. N. C. Designing the next generation of medicines for malaria control and eradication. *Malaria J.* **2013**, *12*, 187.
- (3) Paguio, M. F.; Bogle, K. L.; Roepe, P. D. Plasmodium falciparum resistance to cytotoxic versus cytostatic effects of chloroquine. *Mol. Biochem. Parasit.* **2011**, *178*, 1–6.
- (4) (a) Goldberg, D. E. Hemoglobin degradation. *Curr. Top. Microbiol.* **2005**, *295*, 275–291. (b) Lew, V. L.; Tiffert, T.; Ginsburg, H. Excess hemoglobin digestion and the osmotic stability of Plasmodium falciparum-infected red blood cells. *Blood* **2003**, *101*, 4189–4194. (c) Mauritz, J. M. A.; Seear, R.; Esposito, A.; Kaminski, C. F.; Skepper, J. N.; Warley, A.; Lew, V. L.; Tiffert, T. X-ray microanalysis investigation of the changes in Na, K, and hemoglobin concentration in Plasmodium falciparum-infected red blood cells. *Biophys. J.* **2011**, *100*, 1438–1445.
- (5) Goldberg, D. E.; Slater, A. F. G.; Cerami, A.; Henderson, G. B. Hemoglobin degradation in the malaria parasite Plasmodium falciparum - an ordered process in a unique organelle. *Proc. Natl. Acad. Sci. U.S.A.* **1990**, *87*, 2931–2935.
- (6) (a) Kaphishnikov, S.; Weiner, A.; Shimoni, E.; Guttmann, P.; Schneider, G.; Dahan-Pasternak, N.; Dzikowski, R.; Leiserowitz, L.; Elbaum, M. Oriented nucleation of hemozoin at the digestive vacuole membrane in Plasmodium falciparum. *Proc. Natl. Acad. Sci. U.S.A.* **2012**, *109*, 11188–11193. (b) Orjhi, A. U. Hemozoin accumulation in Gametocyte bodies of Plasmodium falciparum gametocytes. *Parasitol. Res.* **2012**, *111*, 2353–2359.
- (7) (a) Bray, P. G.; Ward, S. A.; O'Neill, P. M. Quinolines and artemisinin: chemistry, biology and history. *Curr. Top. Microbiol.* **2005**, *295*, 3–38. (b) Egan, T. J.; Hunter, R.; Kaschula, C. H.; Marques, H. M.; Misplon, A.; Walden, J. Structure–function relationships in aminoquinolines: Effect of amino and chloro groups on quinoline–hematin complex formation, inhibition of β -hematin formation, and antiparasitic activity. *J. Med. Chem.* **2000**, *43*, 283–291.
- (8) Ecker, A.; Lehane, A. M.; Clain, J.; Fidock, D. A. PfCRT and its role in antimalarial drug resistance. *Trends Parasitol.* **2012**, *28*, 504–514.
- (9) (a) Gligorijevic, B.; McAllister, R.; Urbach, J. S.; Roepe, P. D. Spinning disk confocal microscopy of live, intraerythrocytic malarial parasites. 1. Quantification of hemozoin development for drug sensitive versus resistant malaria. *Biochemistry* **2006**, *45*, 12400–12410. (b) Combrinck, J. M.; Mabotha, T. E.; Ncokazi, K. K.; Ambele, M. A.; Taylor, D.; Smith, P. J.; Hoppe, H. C.; Egan, T. J. Insights into the role of heme in the mechanism of action of antimalarials. *ACS Chem. Biol.* **2013**, *8*, 133–137.
- (10) Gorka, A. P.; de Dios, A.; Roepe, P. D. Quinoline drug–heme interactions and implications for antimalarial cytostatic versus cytotoxic activities. *J. Med. Chem.* **2013**, *56*, 5231–5246.
- (11) (a) de Dios, A. C.; Tycko, R.; Ursos, L. M. B.; Roepe, P. D. NMR studies of chloroquine–ferriprotoporphyrin IX complex. *J. Phys. Chem. A* **2003**, *107*, 5821–5825. (b) de Villiers, K. A.; Marques, H. M.; Egan, T. J. The crystal structure of halofantrine–ferriprotoporphyrin IX and the mechanism of action of arylmethanol antimalarials. *J. Inorg. Biochem.* **2008**, *102*, 1660–1667. (c) Kuter, D.; Chibale, K.; Egan, T. J. Linear free energy relationships predict coordination and π -stacking interactions of small molecules with ferriprotoporphyrin IX. *J. Inorg. Biochem.* **2011**, *105*, 684–692. (d) Asghari-Khiavi, M.; Vongsvivut, J.; Perepichka, I.; Mechler, A.; Wood, B. R.; McNaughton, D.; Bohle, D. S. Interaction of quinoline antimalarial drugs with ferriprotoporphyrin IX, a solid state spectroscopy study. *J. Inorg. Biochem.* **2011**, *105*, 1662–1669.
- (12) (a) Leed, A.; DuBay, K.; Ursos, L. M. B.; Sears, D.; de Dios, A. C.; Roepe, P. D. Solution structures of antimalarial drug–heme complexes. *Biochemistry* **2002**, *41*, 10245–10255. (b) de Dios, A. C.; Casabianca, L. B.; Kosar, A.; Roepe, P. D. Structure of the amodiaquine–FPIX μ oxo dimer solution complex at atomic resolution. *Inorg. Chem.* **2004**, *43*, 8078–8084.
- (13) (a) Buller, R.; Peterson, M. L.; Almarsson, O.; Leiserowitz, L. Quinoline binding site on malaria pigment crystal: A rational pathway for antimalarial drug design. *Cryst. Growth Des.* **2002**, *2*, 553–562. (b) Weissbuch, I.; Leiserowitz, L. Interplay between malaria, crystalline hemozoin formation, and antimalarial drug action and design. *Chem. Rev.* **2008**, *108*, 4899–4914.
- (14) Gorka, A. P.; Alumasa, J. N.; Sherlach, K. S.; Jacobs, L. M.; Nickley, K. B.; Brower, J. P.; de Dios, A. C.; Roepe, P. D. Cytostatic versus cytotoxic activities of chloroquine analogues and inhibition of hemozoin crystal growth. *Antimicrob. Agents Chemother.* **2013**, *57*, 356–364.
- (15) Gildenhuys, J.; le Roex, T.; Egan, T. J.; de Villiers, K. A. The single crystal X-ray structure of β -hematin DMSO solvate grown in the presence of chloroquine, a β -hematin growth-rate inhibitor. *J. Am. Chem. Soc.* **2013**, *135*, 1037–1047.
- (16) Solomonov, I.; Osipova, M.; Feldman, Y.; Baetz, C.; Kjaer, K.; Robinson, I. K.; Webster, G. T.; McNaughton, D.; Wood, B. R.; Weissbuch, I.; Leiserowitz, L. Crystal nucleation, growth, and morphology of the synthetic malaria pigment β -hematin and the effect thereon by quinoline additives: The malaria pigment as a target of various antimalarial drugs. *J. Am. Chem. Soc.* **2007**, *129*, 2615–2627.
- (17) (a) Lavrado, J.; Paulo, A.; Gut, J.; Rosenthal, P. J.; Moreira, R. Cryptolepine analogues containing basic aminoalkyl side-chains at C-11: Synthesis, antiparasitic activity, and cytotoxicity. *Bioorg. Med. Chem. Lett.* **2008**, *18*, 1378–1381. (b) Lavrado, J.; Cabal, G. G.; Prudencio, M.; Mota, M. M.; Gut, J.; Rosenthal, P. J.; Diaz, C.; Guedes, R. C.; dos Santos, D. J. V. A.; Bichenkova, E.; Douglas, K. T.; Moreira, R.; Paulo, A. Incorporation of basic side chains into cryptolepine scaffold: Structure–antimalarial activity relationships and mechanistic studies. *J. Med. Chem.* **2011**, *54*, 734–750.
- (18) Silva, L. F. R. E.; Montoia, A.; Amorim, R. C. N.; Melo, M. R.; Henrique, M. C.; Nunomura, S. M.; Costa, M. R. F.; Neto, V. F. A.; Costa, D. S.; Dantas, G.; Lavrado, J.; Moreira, R.; Paulo, A.; Pinto, A. C.; Tadei, W. P.; Zacardi, R. S.; Eberlin, M. N.; Pohlit, A. M. Comparative in vitro and in vivo antimalarial activity of the indole alkaloids ellipticine, olivacine, cryptolepine and a synthetic cryptolepine analog. *Phytomedicine* **2013**, *20*, 71–76.
- (19) Lavrado, J.; Gani, K.; Nobre, P. A.; Santos, S. A.; Figueiredo, P.; Lopes, D.; do Rosario, V.; Gut, J.; Rosenthal, P. J.; Moreira, R.; Paulo, A. Bis-alkylamine quindolone derivatives as new antimalarial leads. *Bioorg. Med. Chem. Lett.* **2010**, *20*, 5634–5637.
- (20) (a) Navia, M. A.; Chaturvedi, P. R. Design principles for orally bioavailable drugs. *Drug Discovery Today* **1996**, *1*, 179–189. (b) Veber, D. F.; Johnson, S. R.; Cheng, H. Y.; Smith, B. R.; Ward, K. W.; Kopple, K. D. Molecular properties that influence the oral bioavailability of drug candidates. *J. Med. Chem.* **2002**, *45*, 2615–2623.
- (21) Hocart, S. J.; Liu, H. Y.; Deng, H. Y.; De, D.; Krogstad, F. M.; Krogstad, D. J. 4-Aminoquinolines active against chloroquine-resistant Plasmodium falciparum: Basis of antiparasite activity and quantitative structure–activity relationship analyses. *Antimicrob. Agents Chemother.* **2011**, *55*, 2233–2244.
- (22) Renčiuk, D.; Zhou, J.; Beaurepaire, L.; Guédin, A.; Bourdoncle, A.; Mergny, J.-L. A FRET-based screening assay for nucleic acid ligands. *Methods* **2012**, *57*, 122–128.
- (23) (a) Terkuile, F.; White, N. J.; Holloway, P.; Pasvol, G.; Krishna, S. Plasmodium falciparum - in vitro studies of the pharmacodynamic properties of drugs used for the treatment of severe malaria. *Exp. Parasitol.* **1993**, *76*, 85–95. (b) Khan, T.; van Brummelen, A. C.;

Parkinson, C. J.; Hoppe, H. C. ATP and luciferase assays to determine the rate of drug action in in vitro cultures of *Plasmodium falciparum*. *Malaria J.* **2012**, *11*, 369.

(24) Sullivan, D. J.; Gluzman, I. Y.; Russell, D. G.; Goldberg, D. E. On the molecular mechanism of chloroquine's antimalarial action. *Proc. Natl. Acad. Sci. U.S.A.* **1996**, *93*, 11865–11870.

(25) Veiga, M. I.; Ferreira, P. E.; Schmidt, B. A.; Ribacke, U.; Bjorkman, A.; Tichopad, A.; Gil, J. P. Antimalarial exposure delays *Plasmodium falciparum* intra-erythrocytic cycle and drives drug transporter genes expression. *PLoS One* **2010**, *5*, e12408.

(26) Wilson, D. W.; Langer, C.; Goodman, C. D.; McFadden, G. I.; Beeson, J. G. Defining the timing of action of antimalarial drugs against *Plasmodium falciparum*. *Antimicrob. Agents Chemother.* **2013**, *57*, 1455–1467.

(27) Meslin, B.; Barnadas, C.; Boni, V.; Latour, C.; De Monbrison, F.; Kaiser, K.; Picot, S. Features of apoptosis in *Plasmodium falciparum* erythrocytic stage through a putative role of PfMCA1 metacaspase-like protein. *J. Infect. Dis.* **2007**, *195*, 1852–1859.

(28) Geary, T. G.; Divo, A. A.; Jensen, J. B. Stage specific actions of antimalarial-drugs on *Plasmodium-falciparum* in culture. *Am. J. Trop. Med. Hyg.* **1989**, *40*, 240–244.

(29) Hanssen, E.; Knoechel, C.; Dearnley, M.; Dixon, M. W. A.; Le Gros, M.; Larabell, C.; Tilley, L. Soft X-ray microscopy analysis of cell volume and hemoglobin content in erythrocytes infected with asexual and sexual stages of *Plasmodium falciparum*. *J. Struct. Biol.* **2012**, *177*, 224–232.

(30) Gligorijevic, B.; Purdy, K.; Elliott, D. A.; Cooper, R. A.; Roepe, P. D. Stage independent chloroquine resistance and chloroquine toxicity revealed via spinning disk confocal microscopy. *Mol. Biochem. Parasit.* **2008**, *159*, 7–23.

(31) (a) O'Neill, P. M.; Park, B. K.; Shone, A. E.; Maggs, J. L.; Roberts, P.; Stocks, P. A.; Biagini, G. A.; Bray, P. G.; Gibbons, P.; Berry, N.; Winstanley, P. A.; Mukhtar, A.; Bonar-Law, R.; Hindley, S.; Bambal, R. B.; Davis, C. B.; Bates, M.; Hart, T. K.; Gresham, S. L.; Lawrence, R. M.; Brigandi, R. A.; Gomez-Delas-Heras, F. M.; Gargallo, D. V.; Ward, S. A. Candidate selection and preclinical evaluation of *N*-tert-butyl isoquine (GSK369796), an affordable and effective 4-aminoquinoline antimalarial for the 21st century. *J. Med. Chem.* **2009**, *52*, 1408–1415. (b) O'Neill, P. M.; Shone, A. E.; Stanford, D.; Nixon, G.; Asadollahy, E.; Park, B. K.; Maggs, J. L.; Roberts, P.; Stocks, P. A.; Biagini, G.; Bray, P. G.; Davies, J.; Berry, N.; Hall, C.; Rimmer, K.; Winstanley, P. A.; Hindley, S.; Bambal, R. B.; Davis, C. B.; Bates, M.; Gresham, S. L.; Brigandi, R. A.; Gomez-de-las-Heras, F. M.; Gargallo, D. V.; Parapini, S.; Vivas, L.; Lander, H.; Taramelli, D.; Ward, S. A. Synthesis, antimalarial activity, and preclinical pharmacology of a novel series of 4'-fluoro- and 4'-chloro analogues of amodiaquine. Identification of a suitable "back-up" compound for *N*-tert-butylisoquine. *J. Med. Chem.* **2009**, *52*, 1828–1844. (c) Pandey, A. V.; Bisht, H.; Babbarwal, V. K.; Srivastava, J.; Pandey, K. C.; Chauhan, V. S. Mechanism of malarial haem detoxification inhibition by chloroquine. *Biochem. J.* **2001**, *355*, 333–338. (d) Vippagunta, S. R.; Dorn, A.; Ridley, R. G.; Vennerstrom, J. L. Characterization of chloroquine-hematin mu-oxo dimer binding by isothermal titration calorimetry. *Biochim. Biophys. Acta, Gen. Subj.* **2000**, *1475*, 133–140. (e) Casabianca, L. B.; An, D.; Natarajan, J. K.; Alumasa, J. N.; Roepe, P. D.; Wolf, C.; de Dios, A. C. Quinine and chloroquine differentially perturb heme monomer-dimer equilibrium. *Inorg. Chem.* **2008**, *47*, 6077–6081.

(32) (a) Ingham, K. C. Application of Jobs method of continuous variation to stoichiometry of protein-ligand complexes. *Anal. Biochem.* **1975**, *68*, 660–663. (b) Huang, C. Y. Determination of binding stoichiometry by the continuous variation method - the Job Plot. *Method Enzymol.* **1982**, *87*, 509–525.

(33) Martinez, A.; Rajapakse, C. S. K.; Naoulou, B.; Kopkalli, Y.; Davenport, L.; Sanchez-Delgado, R. A. The mechanism of antimalarial action of the ruthenium(II)-chloroquine complex [RuCl₂(CQ)]₂. *J. Biol. Inorg. Chem.* **2008**, *13*, 703–712.

(34) Basilico, N.; Pagani, E.; Monti, D.; Olliaro, P.; Taramelli, D. A microtitre-based method for measuring the haem polymerization

inhibitory activity (HPIA) of antimalarial drugs. *J. Antimicrob. Chemother.* **1998**, *42*, 55–60.

(35) Carvalho, P. A.; Coelho, L.; Martins, R.; Nogueira, F. Differences between synthetic β -haematin and native hemozoin crystals. *Microsc. Microanal.* **2013**, *19* (Suppl 4), 49–50.

(36) Parapini, S.; Basilico, N.; Pasini, E.; Egan, T. J.; Olliaro, P.; Taramelli, D.; Monti, D. Standardization of the physicochemical parameters to assess in vitro the beta-hematin inhibitory activity of antimalarial drugs. *Exp. Parasitol.* **2000**, *96*, 249–256.

(37) Wang, N.; Wicht, K. J.; Wang, L.; Lu, W. J.; Misumi, R.; Wang, M. Q.; El Gokha, A. A. A.; Kaiser, M.; El Sayed, I. E.; Egan, T. J.; Inokuchi, T. Synthesis and in vitro testing of antimalarial activity of non-natural-type neocryptolepines: Structure-activity relationship study of 2,11- and 9,11-disubstituted 6-methylindolo[2,3-b]quinolines. *Chem. Pharm. Bull.* **2013**, *61*, 1282–1290.

(38) Orjih, A. U. Heme polymerase activity and the stage specificity of antimalarial action of chloroquine. *J. Pharmacol. Exp. Ther.* **1997**, *282*, 108–112.

(39) (a) Egan, T. J.; Chen, J. Y. J.; de Villiers, K. A.; Mabotha, T. E.; Naidoo, K. J.; Ncokazi, K. K.; Langford, S. J.; McNaughton, D.; Pandiancherri, S.; Wood, B. R. Haemozoin (β -haematin) biomineralization occurs by self-assembly near the lipid/water interface. *FEBS Lett.* **2006**, *580*, S105–S110. (b) Hoang, A. N.; Ncokazi, K. K.; de Villiers, K. A.; Wright, D. W.; Egan, T. J. Crystallization of synthetic haemozoin ([β]-haematin) nucleated at the surface of lipid particles. *Dalton Trans.* **2010**, *39*, 1235–1244.

(40) Pisciotto, J. M.; Coppens, J.; Tripathi, A. K.; Scholl, P. F.; Shuman, J.; Bajad, S.; Shulaev, V.; Sullivan, D. J. The role of neutral lipid nanospheres in *Plasmodium falciparum* haem crystallization. *Biochem. J.* **2007**, *402*, 197–204.

(41) Warhurst, D. C.; Craig, J. C.; Adagu, P. S.; Guy, R. K.; Madrid, P. B.; Fivelman, Q. L. Activity of piperazine and other 4-aminoquinoline antiparasitodal drugs against chloroquine-sensitive and resistant blood-stages of *Plasmodium falciparum* - role of beta-haematin inhibition and drug concentration in vacuolar water- and lipid-phases. *Biochem. Pharmacol.* **2007**, *73*, 1910–1926.

(42) Dubar, F.; Egan, T. J.; Pradines, B.; Kuter, D.; Ncokazi, K. K.; Forge, D.; Paul, J. F.; Pierrot, C.; Kalamou, H.; Khalife, J.; Buisine, E.; Rogier, C.; Vezin, H.; Forfar, I.; Slomian, C.; Trivelli, X.; Kapishnikov, S.; Leiserowitz, L.; Dive, D.; Biot, C. The antimalarial ferroquine: Role of the metal and intramolecular hydrogen bond in activity and resistance. *ACS Chem. Biol.* **2011**, *6*, 275–287.

(43) (a) Warhurst, D. C.; Steele, J. C. P.; Adagu, I. S.; Craig, J. C.; Cullander, C. Hydroxychloroquine is much less active than chloroquine against chloroquine-resistant *Plasmodium falciparum*, in agreement with its physicochemical properties. *J. Antimicrob. Chemother.* **2003**, *52*, 188–193. (b) Salas, P. F.; Herrmann, C.; Cawthray, J. F.; Nimphius, C.; Kenkel, A.; Chen, J.; de Kock, C.; Smith, P. J.; Patrick, B. O.; Adam, M. J.; Orvig, C. Structural characteristics of chloroquine-bridged ferrocenophane analogues of ferroquine may obviate malaria drug-resistance mechanisms. *J. Med. Chem.* **2013**, *56*, 1596–1613.

(44) Hoang, A. N.; Sandlin, R. D.; Omar, A.; Egan, T. J.; Wright, D. W. The neutral lipid composition present in the digestive vacuole of *Plasmodium falciparum* concentrates heme and mediates β -hematin formation with an unusually low activation energy. *Biochemistry* **2010**, *49*, 10107–10116.

(45) Pasternack, R. F.; Munda, B.; Bickford, A.; Gibbs, E. J.; Sclaro, L. M. On the kinetics of formation of hemozoin, the malaria pigment. *J. Inorg. Biochem.* **2010**, *104*, 1119–1124.

(46) Kapishnikov, S.; Berthing, T.; Hviid, L.; Dierolf, M.; Menzel, A.; Pfeiffer, F.; Als-Nielsen, J.; Leiserowitz, L. Aligned hemozoin crystals in curved clusters in malarial red blood cells revealed by nanoprobe X-ray Fe fluorescence and diffraction. *Proc. Natl. Acad. Sci. U.S.A.* **2012**, *109*, 11184–11187.

(47) Kapishnikov, S.; Weiner, A.; Shimoni, E.; Schneider, G.; Elbaum, M.; Leiserowitz, L. Digestive vacuole membrane in *Plasmodium falciparum*-infected erythrocytes: Relevance to templated nucleation of hemozoin. *Langmuir* **2013**, *29*, 14595–14602.

- (48) Pagola, S.; Stephens, P. W.; Bohle, D. S.; Kosar, A. D.; Madsen, S. K. The structure of malaria pigment beta-haematin. *Nature* **2000**, *404*, 307–310.
- (49) Chen, M. M.; Shi, L. R.; Sullivan, D. J. Haemoproteus and Schistosoma synthesize heme polymers similar to Plasmodium hemozoin and beta-hematin. *Mol. Biochem. Parasit.* **2001**, *113*, 1–8.
- (50) Nogueira, F.; Diez, A.; Radfar, A.; Perez-Benavente, S.; do Rosario, V. E.; Puyet, A.; Bautista, J. M. Early transcriptional response to chloroquine of the Plasmodium falciparum antioxidant defence in sensitive and resistant clones. *Acta Trop.* **2010**, *114*, 109–115.
- (51) Egan, T. J.; Mavuso, W. W.; Ross, D. C.; Marques, H. M. Thermodynamic factors controlling the interaction of quinoline antimalarial drugs with ferriprotoporphyrin IX. *J. Inorg. Biochem.* **1997**, *68*, 137–145.